

# SuperM2M: Supervised and Mixture-to-Mixture Co-Learning for Speech Enhancement and Robust ASR

Zhong-Qiu Wang<sup>a</sup>

<sup>a</sup>Department of Computer Science and Engineering, Southern University of Science and Technology, Shenzhen, 518055, Guangdong, P.R. China

## Abstract

The current dominant approach for neural speech enhancement is based on supervised learning by using simulated training data. The trained models, however, often exhibit limited generalizability to real-recorded data. To address this, this paper investigates training enhancement models directly on real target-domain data. We propose to adapt mixture-to-mixture (M2M) training, originally designed for speaker separation, for speech enhancement, by modeling multi-source noise signals as a single, combined source. In addition, we propose a co-learning algorithm that improves M2M with the help of supervised algorithms. When paired close-talk and far-field mixtures are available for training, M2M realizes speech enhancement by training a deep neural network (DNN) to produce speech and noise estimates in a way such that they can be linearly filtered to reconstruct the close-talk and far-field mixtures. This way, the DNN can be trained directly on real mixtures, and can leverage close-talk and far-field mixtures as a weak supervision to enhance far-field mixtures. To improve M2M, we combine it with supervised approaches to co-train the DNN, where mini-batches of real close-talk and far-field mixture pairs and mini-batches of simulated mixture and clean speech pairs are alternately fed to the DNN, and the loss functions are respectively (a) the mixture reconstruction loss on the real close-talk and far-field mixtures and (b) the regular enhancement loss on the simulated clean speech and noise. We find that, this way, the DNN can learn from real and simulated data to achieve better generalization to real data. We name this algorithm SuperM2M (supervised and mixture-to-mixture co-learning). Evaluation results on the CHiME-4 dataset show its effectiveness and potential.

**Keywords:** Neural speech enhancement, robust ASR

## 1. Introduction

Deep learning has dramatically advanced speech enhancement [1]. The current dominant approach is based on supervised learning, where clean speech is synthetically mixed with noises in simulated reverberant conditions to create paired clean speech and noisy-reverberant mixtures for training neural speech enhancement models in a supervised, discriminative way to predict the clean speech from its paired mixture [1]. Although showing strong performance in matched simulated test conditions [2, 3, 4, 5, 6, 7, 8, 9, 10, 11, 12, 13, 14, 15, 16, 17, 18, 19, 20, 21, 22, 23, 24, 25], the trained models often exhibit limited generalizability to real-recorded data [1, 26, 27, 28, 29, 30, 31, 32, 33, 24, 25, 34], largely due to mismatches between simulated training and real-recorded test conditions.

A possible way to improve the generalizability, we think, is to have the model see, and learn to model, real-recorded target-domain mixtures during training. This, however, cannot be applied in a straightforward way, since the clean speech at each sample of the real mixtures cannot be annotated or computed in an easy way. As a result, there lacks a good sample-level supervision for real mixtures, unlike simulated mixtures where a sample-level supervision is readily available.

During data collection, multiple far-field microphones are usually utilized to record target speakers. In UNSSOR [35], our recent algorithm proposed for unsupervised speaker separation, we find that the mixture signal recorded by each far-field microphone can be leveraged as a *weak supervision* for training DNNs to separate speakers. The idea is that each far-field mixture can be utilized as a constraint to regularize speaker estimates. That is, the speaker estimates, produced by using the mixtures captured at a subset of microphones as input, should be capable of being leveraged to reconstruct the mixture captured by each microphone.

On the other hand, during data collection, besides using far-field microphones to record target speech, a close-talk microphone is often placed near the target speaker to collect its close-talk speech (e.g., in the CHiME [36], AMI [37], AliMeeting [38], and MISP [39] setup).<sup>1</sup> See Fig. 1 for an illustration. Although the close-talk microphone can also pick up non-target signals, the recorded close-talk mixture typically has a much higher signal-to-noise ratio (SNR) of the target speaker than any far-field mixtures. In our recent mixture to mixture (M2M) algorithm [40], which builds upon UNSSOR, we find that, besides far-field mixtures, the close-talk mixture can also be lever-

<sup>1</sup>Close-talk speech is almost always recorded together with far-field speech in speech separation and recognition datasets, as it is much easier for humans to annotate word transcriptions and speaker activities based on close-talk recordings (where the target speech is very strong) than far-field recordings.

Email address: wang.zhongqiu41@gmail.com (Zhong-Qiu Wang)

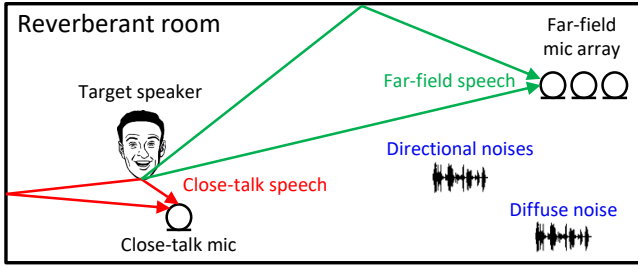


Figure 1: Task illustration. Close-talk mixture consists of close-talk speech and non-target signals. Far-field mixture consists of far-field speech and non-target signals. Best in color.

aged as a *weak supervision* for training DNNs to separate mixed speakers.

To leverage the weak-supervision in far-field and close-talk mixtures for separation, two difficulties need to be solved. First, far-field mixtures contain multiple sources and are not clean, and due to the contamination of the other sources [37, 36, 41], close-talk mixtures are often not clean enough. Second, each speaker’s image in the close-talk mixture is not time-aligned with its image in each far-field mixture, and each speaker’s images in different far-field mixtures are also not time-aligned with each other. As a result, close-talk and far-field mixtures cannot be naively used as the training targets for training speaker separation models. To overcome the two difficulties, we have recently proposed UNSSOR in a conference publication [35] and M2M in a letter submission [40]. The idea is that, at each training step, we can (a) feed a far-field mixture to a DNN to produce an estimate for each speaker; and (b) regularize the speaker estimates such that they can be linearly filtered via multi-frame linear filtering to reconstruct the close-talk and far-field mixtures. This way, the first difficulty is addressed by having the filtered speaker estimates to respectively approximate (i.e., explain) the speaker images in each mixture, and the second difficulty is addressed by multi-frame linear filtering.

Although UNSSOR and M2M are capable of being trained directly on real-recorded mixtures (i.e., not requiring the availability of clean speech), they have been only trained and evaluated on simulated mixtures [35, 40]. It is yet unknown (a) whether they are effective on real data; and (b) whether they can lead to better generalization to real data, compared with the current dominant purely-supervised approaches, which train models only on simulated data. We emphasize that these two concerns are very reasonable, since, on real data, the physical models hypothesized in UNSSOR and M2M are expected to be much less satisfied. For example, there could be microphone synchronization errors, microphone failures, different frequency responses in different microphones, signal clipping, slight speaker and array movement, non-linear filter relationships among speaker images at different microphones, distortions to target speech caused by real microphones, etc. These issues can potentially pose difficulties for UNSSOR and M2M. In addition, UNSSOR and M2M were designed for separating mixed speakers. It is unclear whether they would be effective for single-speaker speech enhancement and robust automatic

speech recognition (ASR), where suppressing non-target signals (such as noises) is a major concern. Furthermore, UNSSOR and M2M assume stationary, weak Gaussian noises in their physical models. It is unclear whether they can deal with strong, non-stationary noises, which could contain an unknown number of diffuse and directional sources.

In this context, we propose to extend UNSSOR [35] and M2M [40] for speech enhancement and robust ASR, where we train and evaluate the proposed algorithms not only on simulated data but also on real data. Our major goal is to show whether the resulting algorithms can yield better generalization to real data than purely-supervised models trained on simulated data, a demonstration that is missing in UNSSOR [35] and M2M [40]. Without this demonstration, the evidence supporting whether this un- and weakly-supervised line of research is worth investigating would be lacking, especially considering the dominance and simplicity of purely-supervised approaches based on simulated training data. We summarize the key contributions of this paper as follows:

- We are the first proposing to leverage close-talk and far-field mixtures as weak supervision for speech enhancement, a task different from speaker separation.
- Considering noise sources as a single, combined source, we propose to formulate the training of speech enhancement models on real data as solving a blind deconvolution problem, following the formulations in UNSSOR [35] and M2M [40] designed for speaker separation.
- We propose SuperM2M, a co-learning strategy which trains the same DNN model by alternating between M2M training on real data and supervised learning on simulated data. This way, M2M can benefit from massive simulated training data, especially when the real training data is scarce. In addition, we find that this strategy can help mitigate the weaknesses of UNSSOR and M2M on source and frequency permutation, and source ambiguity (which we will detail in Section 4.5).

We validate SuperM2M on the CHiME-4 dataset [42], which is consisted of simulated and challenging real-recorded mixtures and is currently the major benchmark for evaluating robust ASR and speech enhancement algorithms. In our experiments, state-of-the-art ASR and enhancement performance is obtained. The evaluation results suggest that:

- SuperM2M can effectively learn from real mixtures and leverage the weak supervision afforded by real close-talk and far-field mixtures.
- The co-learning strategy can significantly improve the generalizability of purely-supervised models trained on simulated data to real data.

The evaluation results provide an experimental evidence supporting the strong potential of our un- and weakly-supervised line of research for speech enhancement. A sound demo is provided in the link below.<sup>2</sup>

<sup>2</sup>[https://zqwang7.github.io/demos/SuperM2M\\_demo/index.html](https://zqwang7.github.io/demos/SuperM2M_demo/index.html)

## 2. Related Work

SuperM2M is related to other work in five major aspects.

### 2.1. Frontend Enhancement and Robust ASR

Leveraging neural speech enhancement as a frontend processing to improve the robustness of backend ASR systems to noise, reverberation and competing speech has been a long-lasting research topic [33, 43]. Although dramatic progress has been made in neural speech enhancement [1, 20], directly feeding the immediate estimate produced by DNN-based enhancement models for ASR has had limited success, largely for two reasons: (a) enhancement DNNs, which can suppress non-target signals aggressively, often incur speech distortion detrimental to ASR; and (b) enhancement DNNs are often trained on simulated data, which inevitably mismatches real data, and this mismatch further aggravates the speech distortion problem. Through years of efforts, robust ASR approaches have gradually converged to (a) leveraging DNN estimates to derive linear beamforming results for ASR [44, 45, 46]; and (b) jointly training ASR models with enhancement models [47, 48, 49, 50]. These two approaches aim at improving robust ASR performance. Their enhancement modules usually do not produce sufficiently accurate estimation of target speech. For example, linear beamforming is known to introduce little speech distortion but it has limited capabilities at suppressing non-target signals (especially when the number of microphones is limited and when the non-target signals are diffuse) [51]. Another example is that jointly training enhancement models with ASR models often degrades the performance of the enhancement models on realistic mixtures [52].

Differently, in this paper we aim at building neural speech enhancement models whose immediate estimate *itself* can have low distortion to target speech and high reduction to non-target signals, especially on real test data. We find that, on the challenging real test data of CHiME-4 [42], the immediate output of SuperM2M bears low distortion to target speech and high reduction to non-target signals, and feeding it directly to strong ASR models for recognition yields strong performance.

### 2.2. Generalizability of Supervised Models to Real Data

Improving the generalizability of neural speech enhancement models to real data has received decade-long efforts. The current dominant approach [2, 1, 24, 25] is to train supervised models on large-scale synthetic data, which is simulated in a way to cover as many variations (that could happen in real test data) as possible. However, the success has been limited, largely due to the current simulation techniques being not good enough at generating simulated mixtures as realistic as real mixtures. This can be observed from recent speech enhancement and ASR challenges. In the Clarity enhancement challenge [30], all the teams scored well on simulated data failed on real data. In CHiME-3/4 [42], in the multi-channel cases, all the top teams use conventional beamformers (although with signal statistics estimated based on DNN estimates) as the only frontend, and

in the single-channel cases, frontend enhancement often degrades ASR performance compared to not using any enhancement (assuming no joint frontend-backend training) [53]. In CHiME-{5,6,7} [41] and M2MeT [38], almost all the teams adopt guided source separation [46], a signal processing algorithm, as the only frontend.

Since the current simulation techniques are not satisfactory enough, a possible way to improve the generalizability to real data, we think, is to train enhancement models directly on real data.

### 2.3. Unsupervised Speech Separation

To model real data, unsupervised neural speech separation algorithms (such as MixIT [54], ReMixIT [28], NyTT [55], Neural FCA [56], RAS [57], UNSSOR [35] and USDnet [58]), which can train separation models directly on mixtures or synthetic mixtures of mixtures, have been proposed. Due to their unsupervised nature, their performance could be limited due to not leveraging any supervision. Meanwhile, many algorithms in this stream are only evaluated on simulated data and their effectiveness on real data and for robust ASR is unclear. In contrast, we will show that SuperM2M works well on the challenging real data of CHiME-4.

### 2.4. Semi-Supervised Speech Separation

A promising direction, suggested by [59, 60] (and subsequent studies [61, 62]), is to combine supervised learning on simulated data and unsupervised learning on real data for model training, forming a semi-supervised approach. The rationale is that supervised learning on massive simulated data offers an easy and feasible way for the model to learn to model speech patterns, and unsupervised learning on real data can help the model learn from real data.

SuperM2M follows this direction, but differs from [59, 60] in two major aspects. First, SuperM2M leverages M2M [40], which builds upon UNSSOR [35], to model real data, while [59, 60] uses MixIT [54]. As is suggested in [35, 58], UNSSOR based methods (a) avoid tricky (and often unrealistic) synthesis of mixtures of mixtures, which, on the other hand, increases the number of sources to separate; (b) are more flexible at multi-channel separation; and (c) can be readily configured to perform dereverberation besides separation [58], while MixIT cannot. On the other hand, when close-talk mixtures are available, M2M can be readily configured weakly-supervised to leverage the weak supervision afforded by close-talk mixtures.

### 2.5. Weakly-Supervised Speech Separation

SuperM2M, building upon UNSSOR [35] and M2M [40], can be configured to leverage close-talk mixtures as a weak supervision to enhance far-field mixtures. In the literature, there are earlier studies on weakly-supervised speech enhancement and source separation. In [63, 64], discriminators, essentially source prior models trained in an adversarial way, are used to help separation models produce separation results with distributions close to clean sources. In [50], separation models

are jointly trained with ASR models to leverage the weak supervision of word transcriptions. In [65], a pre-trained sound classifier is employed to check whether separated signals can be classified into target sound classes, thereby promoting separation. These approaches require clean sources, human annotations (e.g., word transcriptions), and source prior models (e.g., discriminators, ASR models, and sound classifiers). In comparison, M2M needs close-talk and far-field mixture pairs, which can be obtained during data collection by using close-talk in addition to far-field microphones, and it does not require source prior models. In addition, close-talk mixtures exploited in M2M can provide a *sample-level* supervision, offering much more fine-grained supervision than source prior models, word transcriptions, and segment-level sound class labels.

### 3. Problem Formulation

We start with describing the hypothesized physical models, then propose to formulate speech enhancement as a blind deconvolution problem, and at last overview the proposed algorithm for speech enhancement.

#### 3.1. Physical Model

In reverberant conditions with a compact far-field  $P$ -microphone array and a single target speaker wearing a close-talk microphone (see Fig. 1 for an illustration), the physical model for each recorded mixture can be formulated, in the short-time Fourier transform (STFT) domain, in the following way.

At a designated reference far-field microphone  $q \in \{1, \dots, P\}$ , the recorded mixture is formulated as

$$\begin{aligned} Y_q(t, f) &= X_q(t, f) + V_q(t, f) \\ &= S_q(t, f) + H_q(t, f) + V_q(t, f) \\ &= S_q(t, f) + \mathbf{g}_q(f)^H \bar{\mathbf{S}}_q(t, f) + V_q(t, f) + \varepsilon_q(t, f), \quad (1) \end{aligned}$$

where  $t$  indexes  $T$  frames,  $f$  indexes  $F$  frequency bins, and  $Y_q(t, f)$ ,  $X_q(t, f)$  and  $V_q(t, f)$  in row 1 are respectively the STFT coefficients of the mixture, reverberant speech of the target speaker, and non-speech signals at time  $t$ , frequency  $f$  and microphone  $q$ . In row 2,  $X_q(t, f)$  is decomposed to direct-path signal  $S_q(t, f)$  and reverberation  $H_q(t, f)$ . In row 3, following narrowband approximation [66, 51], reverberation  $H_q(\cdot, f)$  is approximated as a linear convolution between the direct-path signal  $S(\cdot, f)$  and a linear filter  $\mathbf{g}_q(f)$ . That is,  $H_q(t, f) \approx \mathbf{g}_q(f)^H \bar{\mathbf{S}}_q(t, f)$ , where  $\bar{\mathbf{S}}_q(t, f) = [\hat{S}_q(t - K + 1, f), \dots, \hat{S}_q(t - \Delta, f)] \in \mathbb{C}^{K-\Delta}$  stacks  $K - \Delta$  T-F units with  $\Delta$  denoting a positive prediction delay,  $\mathbf{g}_q(f) \in \mathbb{C}^{K-\Delta}$  can be interpreted as the relative transfer function (RTF) relating the direct-path signal to the reverberation of the target speaker, and  $(\cdot)^H$  computes Hermitian transpose. In row 3,  $\varepsilon_q(\cdot, f)$  denotes the modeling error incurred by narrowband approximation. In the rest of this paper, when dropping indices  $t$  and  $f$ , we refer to the corresponding spectrograms. We emphasize that  $V_q$  could contain multiple strong, non-stationary directional as well as diffuse noises. In this paper, we model them using a single, combined source.

At any non-reference far-field microphone  $p \in \{1, \dots, P\}$ , where  $p \neq q$ , we formulate the physical model as

$$\begin{aligned} Y_p(t, f) &= X_p(t, f) + V_p(t, f) \\ &= \mathbf{h}_p(f)^H \bar{\mathbf{S}}_q(t, f) + V_p(t, f) + \varepsilon_p(t, f) \\ &= \mathbf{h}_p(f)^H \bar{\mathbf{S}}_q(t, f) + \mathbf{r}_p(f)^H \hat{\mathbf{V}}_q(t, f) + \varepsilon'_p(t, f). \quad (2) \end{aligned}$$

In row 2, we use narrowband approximation, similarly to (1), to approximate  $X_p(t, f) \approx \mathbf{h}_p(f)^H \bar{\mathbf{S}}_q(t, f)$ , where  $\bar{\mathbf{S}}_q(t, f) = [S_q(t - \hat{I} + 1, f), \dots, S_q(t + \hat{J}, f)] \in \mathbb{C}^{\hat{I}+\hat{J}}$  and  $\mathbf{h}_p(f) \in \mathbb{C}^{\hat{I}+\hat{J}}$ , and we use  $\varepsilon_p$  to denote the modeling error.  $\mathbf{h}_p(f)$  can be interpreted as the RTF relating the direct-path signal  $S_q$  (captured by the reference microphone  $q$ ) to the speaker image at another far-field microphone  $p$  (i.e.,  $X_p$ ). In row 3, we use the same trick to approximate non-speech signals  $V_p(t, f) \approx \mathbf{r}_p(f)^H \hat{\mathbf{V}}_q(t, f)$ , where  $\hat{\mathbf{V}}_q(t, f) = [V_q(t - \hat{I} + 1, f), \dots, V_q(t + \hat{J}, f)] \in \mathbb{C}^{\hat{I}+\hat{J}}$ ,  $\mathbf{r}_p(f) \in \mathbb{C}^{\hat{I}+\hat{J}}$ , and  $\varepsilon'_p$  absorbs the incurred modeling error and  $\varepsilon_p$ . Notice that, for simplicity, we use  $\hat{I} - 1$  past and  $\hat{J}$  future taps for both  $\bar{\mathbf{S}}_q(t, f)$  and  $\hat{\mathbf{V}}_q(t, f)$ , although it might be better to use different taps for different sources. On the other hand,  $\mathbf{r}_p(f)^H \hat{\mathbf{V}}_q(t, f)$  could be a crude approximation of  $V_p(t, f)$ , as there could be multiple directional and diffuse noise sources, rather than a single directional speaker source like in  $S_q$ .

Following (2), the closed-talk mixture is formulated as follows:

$$\begin{aligned} Y_0(t, f) &= X_0(t, f) + V_0(t, f) \\ &= \mathbf{h}_0(f)^H \check{\mathbf{S}}_q(t, f) + V_0(t, f) + \varepsilon_0(t, f) \\ &= \mathbf{h}_0(f)^H \check{\mathbf{S}}_q(t, f) + \mathbf{r}_0(f)^H \hat{\mathbf{V}}_q(t, f) + \varepsilon'_0(t, f), \quad (3) \end{aligned}$$

where we use subscript 0 to denote the close-talk microphone and differentiate it with far-field microphones. In row 2,  $X_0(t, f) \approx \mathbf{h}_0(f)^H \check{\mathbf{S}}_q(t, f)$  with  $\check{\mathbf{S}}_q(t, f) = [S_q(t - \check{I} + 1, f), \dots, S_q(t + \check{J}, f)] \in \mathbb{C}^{\check{I}+\check{J}}$  and  $\mathbf{h}_0(f) \in \mathbb{C}^{\check{I}+\check{J}}$ . In row 3,  $V_0(t, f) \approx \mathbf{r}_0(f)^H \hat{\mathbf{V}}_q(t, f)$ , with  $\hat{\mathbf{V}}_0(t, f) = [V_q(t - \hat{I} + 1, f), \dots, V_q(t + \hat{J}, f)] \in \mathbb{C}^{\hat{I}+\hat{J}}$  and  $\mathbf{r}_0(f) \in \mathbb{C}^{\hat{I}+\hat{J}}$ . In  $X_0$ , the direct-path signal of the target speaker is often much stronger than its reverberation, and hence  $X_0$  can be largely viewed as the dry source signal. In this case,  $\mathbf{h}_0(f)$  can be interpreted as a deconvolutional filter that can reverse the time delay and gain decay in the direct-path signal  $S_q$  to recover the speech source signal.

#### 3.2. Formulating Speech Enhancement as Blind Deconvolution

As is suggested by UNSSOR [35] and M2M [40], close-talk and far-field mixtures contain weak supervision for speaker separation. One way to exploit the weak supervision for speech enhancement is by solving the following problem, which finds sources,  $S_q(\cdot, \cdot)$  and  $V_q(\cdot, \cdot)$ , and filters,  $\mathbf{g}_q(\cdot)$ ,  $\mathbf{h}_p(\cdot)$  and  $\mathbf{r}_p(\cdot)$ , that

are most consistent with the physical models in (1), (2) and (3):

$$\begin{aligned} & \underset{\substack{S_q(\cdot, \cdot), V_q(\cdot, \cdot), \\ \mathbf{g}_q(\cdot), \mathbf{h}(\cdot), \mathbf{r}(\cdot)}}{\operatorname{argmin}} \left( \sum_{t,f} |Y_q(t, f) - S_q(t, f) - \mathbf{g}_q(f)^H \widetilde{\mathbf{S}}_q(t, f) - V_q(t, f)|^2 \right. \\ & + \sum_{p=1, p \neq q}^P \sum_{t,f} |Y_p(t, f) - \mathbf{h}_p(f)^H \widetilde{\mathbf{S}}_q(t, f) - \mathbf{r}_p(f)^H \hat{V}_q(t, f)|^2 \\ & \left. + \sum_{t,f} |Y_0(t, f) - \mathbf{h}_0(f)^H \check{\mathbf{S}}_q(t, f) - \mathbf{r}_0(f)^H \hat{V}_q(t, f)|^2 \right), \quad (4) \end{aligned}$$

where  $|\cdot|$  computes magnitude. This is a blind deconvolution problem [67], which is non-convex and difficult to be solved since the speech source, noise source, and linear filters are all unknown and need to be estimated. It is known not solvable if no prior knowledge is assumed about the sources or filters.

In [35], UNSSOR, which models source priors via unsupervised deep learning, is proposed to tackle this category of blind deconvolution problems. It is shown effective at separating reverberant multi-speaker mixtures to reverberant speaker images in simulated conditions.

### 3.3. Overview of Adapting M2M for Speech Enhancement

Building upon the preliminary successes of UNSSOR [35] and M2M [40] in speaker separation on simulated data, this paper adapts M2M training for neural speech enhancement and performs training and evaluation on real-recorded data. The high-level idea is to use un- or weakly-supervised deep learning to first estimate the speech and noise sources. With the two sources estimated, filter estimation in (4) becomes much simpler linear regression problems, where closed-form solutions exist and can be readily computed. With the sources and filters estimated, we can then compute a loss defined similarly to the objective in (4) to regularize the two source estimates to have them respectively approximate the speech and noise sources.

## 4. M2M for Speech Enhancement

Fig. 2(a) illustrates M2M training for speech enhancement. The DNN takes in far-field mixtures as input and produces an estimate  $\hat{S}_q$  for the target speaker and an estimate  $\hat{V}_q$  for non-target signals. Each estimate is then linearly filtered via forward convolutive prediction [68] to optimize a so-called mixture-constraint loss, which encourages the filtered estimates to add up to the close-talk mixture and each far-field mixture, thereby exploiting the weak supervision afforded by close-talk and far-field mixtures for enhancement.

This section describes the DNN setup, loss functions, FCP filtering, as well as the weaknesses of M2M, which lead to the design of SuperM2M. To avoid confusion, in Table 1 we list the major hyper-parameters we will use to describe M2M.

### 4.1. DNN Configurations

The DNN is trained to perform complex spectral mapping [13, 14, 15], where the real and imaginary (RI) components of far-field mixtures are stacked as input features for the DNN to

predict the RI components of  $\hat{S}_q$  and  $\hat{V}_q$ . The DNN setup is described later in Section 6.5, and the loss function next. We can optionally apply iSTFT-STFT projection to  $\hat{S}_q$  and  $\hat{V}_q$  before loss computation (see later Section 6.7.2 for details).

### 4.2. Mixture-Constraint Loss

Following UNSSOR [35], M2M [40] and the objective in (4), we propose the following mixture-constraint (MC) loss, which regularizes the DNN estimates  $\hat{S}_q$  and  $\hat{V}_q$  to have them respectively approximate  $S_q$  and  $V_q$ , by checking whether they can be utilized to reconstruct the recorded mixtures:

$$\mathcal{L}_{\text{MC}} = \mathcal{L}_{\text{MC},q} + \frac{1}{P-1} \times \sum_{p=1, p \neq q}^P \mathcal{L}_{\text{MC},p} + \mathcal{L}_{\text{MC},0}, \quad (5)$$

where the three terms respectively follow the ones in (4) and are detailed next.

$\mathcal{L}_{\text{MC},q}$ , following the first term in (4), is the MC loss at the reference far-field microphone  $q$ :

$$\begin{aligned} \mathcal{L}_{\text{MC},q} &= \sum_{t,f} \mathcal{F}(Y_q(t, f), \hat{Y}_q(t, f)) \\ &= \sum_{t,f} \mathcal{F}(Y_q(t, f), \hat{S}_q(t, f) + \hat{H}_q(t, f) + \hat{V}_q(t, f)) \\ &= \sum_{t,f} \mathcal{F}(Y_q(t, f), \hat{S}_q(t, f) + \hat{\mathbf{g}}_q(f)^H \widetilde{\mathbf{S}}_q(t, f) + \hat{V}_q(t, f)). \end{aligned} \quad (6)$$

In row 2, the DNN estimates  $\hat{S}_q$  and  $\hat{V}_q$  are utilized to reconstruct the mixture  $Y_q$  via  $\hat{Y}_q = \hat{S}_q + \hat{H}_q + \hat{V}_q$ , with the reverberation of the target speaker,  $\hat{H}_q$ , estimated by reverberating  $\hat{S}_q$  via  $\hat{H}_q(t, f) = \hat{\mathbf{g}}_q(f)^H \widetilde{\mathbf{S}}_q(t, f)$ , where  $\widetilde{\mathbf{S}}_q(t, f) = [\hat{S}_q(t - K + 1, f), \dots, \hat{S}_q(t - \Delta, f)]^T \in \mathbb{C}^{K-\Delta}$  stacks a window of past T-F units with a positive prediction delay  $\Delta$ , and  $\hat{\mathbf{g}}_q(f) \in \mathbb{C}^{K-\Delta}$  is an estimated FCP filter to be described later in Section 4.3.  $\mathcal{F}(\cdot, \cdot)$ , to be described in (9), is a distance function.

Similarly,  $\mathcal{L}_{\text{MC},p}$ , following the second term in (4), is the MC loss at each non-reference far-field microphone  $p$ :

$$\begin{aligned} \mathcal{L}_{\text{MC},p} &= \sum_{t,f} \mathcal{F}(Y_p(t, f), \hat{Y}_p(t, f)) \\ &= \sum_{t,f} \mathcal{F}(Y_p(t, f), \hat{X}_p(t, f) + \hat{V}_p(t, f)) \\ &= \sum_{t,f} \mathcal{F}(Y_p(t, f), \hat{\mathbf{h}}_p(f)^H \widetilde{\mathbf{S}}_q(t, f) + \hat{\mathbf{r}}_p(f)^H \hat{V}_q(t, f)), \end{aligned} \quad (7)$$

where  $\hat{X}_p(t, f) = \hat{\mathbf{h}}_p(f)^H \widetilde{\mathbf{S}}_q(t, f)$ , with  $\widetilde{\mathbf{S}}_q(t, f) = [\hat{S}_q(t - i + 1, f), \dots, \hat{S}_q(t + j, f)]^T \in \mathbb{C}^{i+j}$  and  $\hat{\mathbf{h}}_p(f) \in \mathbb{C}^{i+j}$ , and  $\hat{V}_p(t, f) = \hat{\mathbf{r}}_p(f)^H \hat{V}_q(t, f)$ , with  $\hat{\mathbf{r}}_p(f) = [\hat{V}_q(t - i + 1, f), \dots, \hat{V}_q(t + j, f)]^T \in \mathbb{C}^{i+j}$  and  $\hat{\mathbf{r}}_p(f) \in \mathbb{C}^{i+j}$ .  $\hat{\mathbf{h}}_p(f)$  and  $\hat{\mathbf{r}}_p(f)$  are both estimated FCP filters to be described in Section 4.3.

Similarly,  $\mathcal{L}_{\text{MC},0}$ , following the third term in (4) and  $\mathcal{L}_{\text{MC},p}$

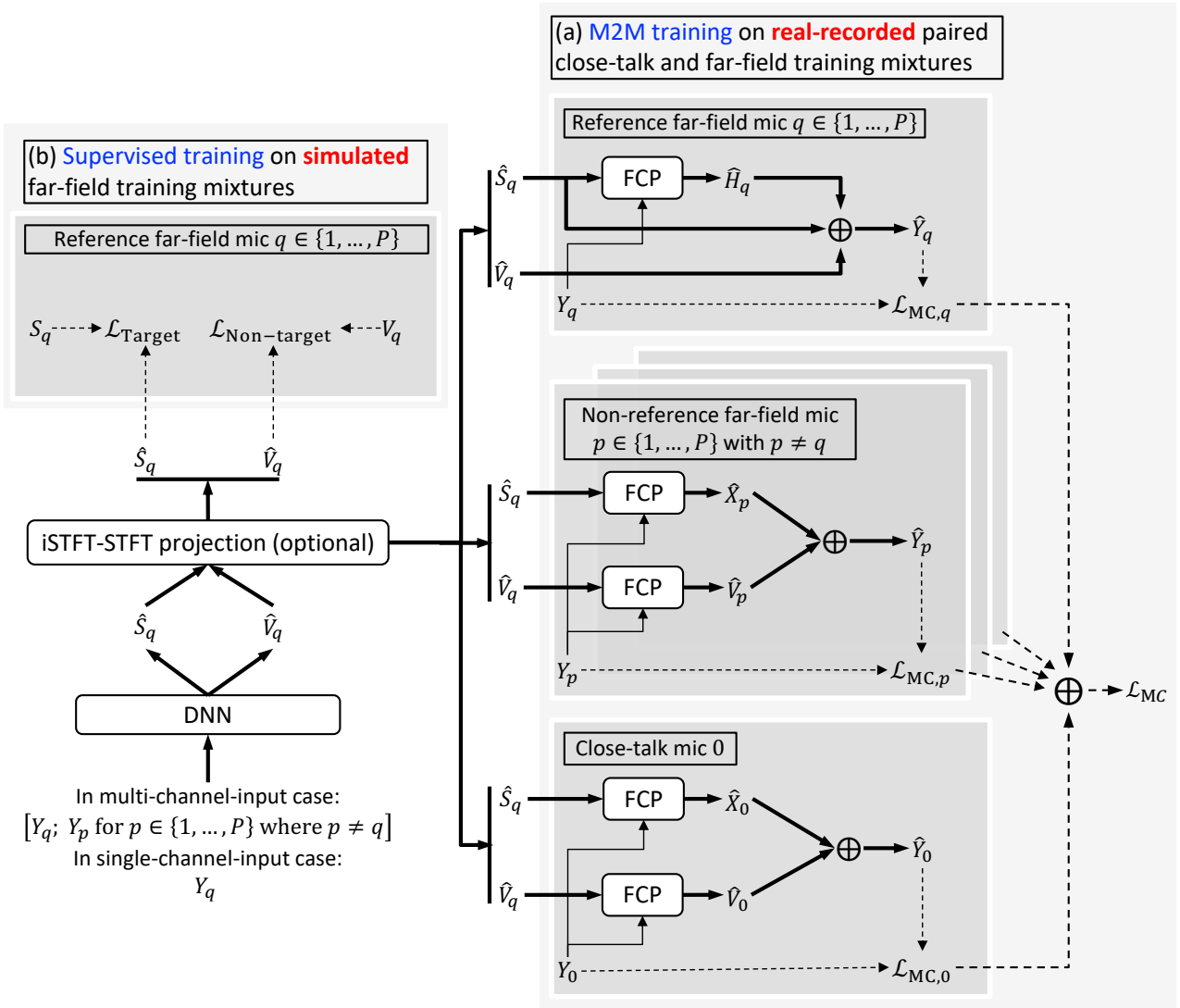


Figure 2: Illustration of SuperM2M, which consists of (a) M2M training on real close-talk and far-field mixture pairs (described in first paragraph of Section 4); and (b) supervised training on simulated far-field mixtures (described in Section 5). M2M trains the DNN to separate far-field mixtures to two sources that can be linearly filtered to reconstruct far-field and close-talk mixtures. In SuperM2M, we alternately feed in mini-batches of real mixtures and mini-batches of simulated mixtures, and train the same DNN by alternating between M2M training on real data and supervised learning on simulated data.

Table 1: Major hyper-parameters of M2M training

Symbols	Description	Eq.	Definition
$K, \Delta$	Past taps & prediction delay for reference far-field mic	(6)	$\tilde{\mathbf{S}}_q(t, f) = [\hat{S}_q(t - K + 1, f), \dots, \hat{S}_q(t - \Delta, f)]^\top \in \mathbb{C}^{K-\Delta}$
$I, J$	Past & future taps for non-reference far-field mics	(7) (7)	$\tilde{\mathbf{S}}_q(t, f) = [\hat{S}_q(t - I + 1, f), \dots, \hat{S}_q(t + J, f)]^\top \in \mathbb{C}^{I+J}$ $\tilde{\mathbf{V}}_q(t, f) = [\hat{V}_q(t - I + 1, f), \dots, \hat{V}_q(t + J, f)]^\top \in \mathbb{C}^{I+J}$
$\check{I}, \check{J}$	Past & future taps for close-talk mic	(8) (8)	$\check{\mathbf{S}}_q(t, f) = [\hat{S}_q(t - \check{I} + 1, f), \dots, \hat{S}_q(t + \check{J}, f)]^\top \in \mathbb{C}^{\check{I}+\check{J}}$ $\check{\mathbf{V}}_q(t, f) = [\hat{V}_q(t - \check{I} + 1, f), \dots, \hat{V}_q(t + \check{J}, f)]^\top \in \mathbb{C}^{\check{I}+\check{J}}$
$\xi$	Weight flooring factor in FCP	(12)	-
$R$	Set of future taps $\Omega = \{0, 1, \dots, R\}$ to enumerate when estimating $J$ on the fly	(13)	-

in (7), is the MC loss at the close-talk microphone:

$$\begin{aligned}
\mathcal{L}_{\text{MC},0} &= \sum_{t,f} \mathcal{F}(Y_0(t, f), \hat{Y}_0(t, f)) \\
&= \sum_{t,f} \mathcal{F}(Y_0(t, f), \hat{X}_0(t, f) + \hat{V}_0(t, f)) \\
&= \sum_{t,f} \mathcal{F}(Y_0(t, f), \hat{\mathbf{h}}_0(f)^H \check{\mathbf{S}}_q(t, f) + \hat{\mathbf{r}}_0(f)^H \check{\mathbf{V}}_q(t, f)), \quad (8)
\end{aligned}$$

where  $\hat{X}_0(t, f) = \hat{\mathbf{h}}_0(f)^H \check{\mathbf{S}}_q(t, f)$ , with  $\check{\mathbf{S}}_q(t, f) = [\hat{S}_q(t - \check{I} + 1, f), \dots, \hat{S}_q(t + \check{J}, f)]^\top \in \mathbb{C}^{\check{I}+\check{J}}$  and  $\hat{\mathbf{h}}_0(f) \in \mathbb{C}^{\check{I}+\check{J}}$ , and  $\hat{V}_0(t, f) = \hat{\mathbf{r}}_0(f)^H \check{\mathbf{V}}_q(t, f)$ , with  $\check{\mathbf{V}}_q(t, f) = [\hat{V}_q(t - \check{I} + 1, f), \dots, \hat{V}_q(t + \check{J}, f)]^\top \in \mathbb{C}^{\check{I}+\check{J}}$  and  $\hat{\mathbf{r}}_0(f) \in \mathbb{C}^{\check{I}+\check{J}}$ .  $\hat{\mathbf{h}}_0(f)$  and  $\hat{\mathbf{r}}_0(f)$  are estimated FCP filters to be described in Section 4.3.

Following [69],  $\mathcal{F}(\cdot, \cdot)$  computes a loss on the estimated RI components and their magnitude:

$$\begin{aligned}
\mathcal{F}(Y_r(t, f), \hat{Y}_r(t, f)) &= \frac{1}{\sum_{r',f'} |Y_{r'}(t', f')|} \mathcal{G}(Y_r(t, f), \hat{Y}_r(t, f)), \quad (9) \\
\mathcal{G}(Y_r(t, f), \hat{Y}_r(t, f)) &= |\mathcal{R}(Y_r(t, f)) - \mathcal{R}(\hat{Y}_r(t, f))| \\
&\quad + |\mathcal{I}(Y_r(t, f)) - \mathcal{I}(\hat{Y}_r(t, f))| \\
&\quad + ||Y_r(t, f)| - |\hat{Y}_r(t, f)||, \quad (10)
\end{aligned}$$

where  $r \in \{0, 1, \dots, P\}$  indexes all the microphones,  $|\cdot|$  computes magnitude,  $\mathcal{R}(\cdot)$  and  $\mathcal{I}(\cdot)$  respectively extract RI components, and the denominator in (9) balances the losses at different microphones and across training mixtures.

Notice that the DNN can use all or a subset of the far-field microphone signals as the input and for loss computation. For example, we can train a monaural enhancement model by just using the reference microphone signal as the input but computing the loss on all the microphone signals.

#### 4.3. FCP for Filter Estimation

To compute  $\mathcal{L}_{\text{MC}}$ , we need to first compute the linear filters (i.e., RTFs) in (6), (7) and (8). Following UNSSOR [35], we leverage FCP [68, 70] for filter estimation, based on the DNN estimates and observed mixtures.

Assuming that the target speaker is non-moving within each utterance, we estimate, e.g., the filter  $\hat{\mathbf{h}}_0(f)$  in (8), by solving the following problem:

$$\hat{\mathbf{h}}_0(f) = \underset{\mathbf{h}_0(f)}{\operatorname{argmin}} \sum_t \frac{1}{\hat{\lambda}_0(t, f)} |Y_0(t, f) - \mathbf{h}_0(f)^H \check{\mathbf{S}}_q(t, f)|^2, \quad (11)$$

where  $\hat{\lambda}$ , to be described in (12), is a weighting term. The objective in (11) is quadratic, where a closed-form solution can be readily computed. We use the same method in (11) (i.e., linearly projecting DNN estimate to observed mixture) to compute all the other filters, and then plug the closed-form solutions to compute the  $\mathcal{L}_{\text{MC}}$  loss and train the DNN.

In (11),  $\hat{\lambda}$  is a weighting term balancing the importance of each T-F unit, as different T-F units usually have diverse energy levels. Following [68], it is defined as

$$\hat{\lambda}_r(t, f) = \xi \times \max(|Y_r|^2) + |Y_r(t, f)|^2, \quad (12)$$

where  $r$  indexes all the microphones,  $\xi$  (tuned to  $10^{-2}$  in this study) floors the weighting term, and  $\max(\cdot)$  extracts the maximum value of a power spectrogram. Notice that we compute  $\hat{\lambda}$  differently for different microphones, as the energy level of each source can be very different at close-talk and far-field microphones, and deployed microphones, even if placed close to each other, often produce very different gain levels in real-world scenarios.

#### 4.4. On-the-fly Estimation of Future Taps $\check{J}$ for Close-Talk Mic

The hyper-parameters for the FCP filter taps in M2M training are listed in Table 1. Their ideal values are likely different for different utterances, while it is tricky and cumbersome to tune each one of them individually for each utterance. For simplicity, in UNSSOR [35] and M2M [40], the value of each hyper-parameter is configured shared for all the training utterances.

This strategy could be improved for real-recorded data, such as CHiME-4 [42]. In CHiME-4, we observe that the far-field microphones are reasonably synchronized as they are placed on, and processed by, the same device, but the close-talk microphone, placed on a different device, is not accurately

synchronized with the far-field microphones and their time-misalignment can be as large as 50 ms. On the other hand, the distance between the far-field microphone array and the close-talk microphone is unknown and can vary from utterance to utterance.

In this context, for simplicity, we set, for all the training utterances,  $\hat{I} = \check{I}$  (the past taps for non-reference far-field microphones and close-talk microphone, described in Table 1) and  $\hat{J} = 1$  (the future taps for non-reference far-field microphones), while we propose to, at each training step, estimate  $\check{J}$  (the future taps for close-talk microphone) for each training utterance in the mini-batch by solving the problem below, which, following the  $\mathcal{L}_{\text{MC},0}$  loss in (8), enumerates a set of future taps and finds the one that leads to the best approximation of the close-talk mixture based on very short FCP filters:

$$\check{J} = \underset{Z \in \Omega}{\operatorname{argmin}} \sum_{t,f} \mathcal{F}(Y_0(t,f), \hat{\mathbf{h}}_0(f)^H \vec{\hat{\mathbf{S}}}_q(t,f) + \hat{\mathbf{r}}_0(f)^H \vec{\hat{\mathbf{V}}}_q(t,f)), \quad (13)$$

where  $\vec{\hat{\mathbf{S}}}_q(t,f) = [\hat{S}_q(t+Z-O+1,f), \dots, \hat{S}_q(t+Z,f)]^T \in \mathbb{C}^O$ ,  $\vec{\hat{\mathbf{V}}}_q(t,f) = [\hat{V}_q(t+Z-O+1,f), \dots, \hat{V}_q(t+Z,f)]^T \in \mathbb{C}^O$ ,  $O$  is set to a small value (3 in this study) so that the filter is short and the amount of computation spent on solving this problem is small,  $\Omega = \{0, 1, \dots, R\}$  denotes a set of future taps to enumerate (with  $R$  tuned to 8 for CHiME-4 to account for potentially large errors in synchronization),  $Z \in \Omega$  denotes an enumerated candidate future tap, and  $\hat{\mathbf{h}}_0(f)$  and  $\hat{\mathbf{r}}_0(f)$  are computed in the same way as in (11).

Note that we run (13) at each training step to estimate  $\check{J}$  for each training utterance in the mini-batch. We stop gradients for the operations in (13) in the forward pass, and no back-propagation is performed for the operations in (13). The estimated  $\check{J}$  is then used for computing the  $\mathcal{L}_{\text{MC},0}$  loss in (8).

#### 4.5. Weaknesses of M2M Training

M2M is a weakly-supervised speech enhancement algorithm that can learn from the weak supervision afforded by close-talk and far-field mixtures. It can also be viewed, with a grain of salt, as an unsupervised enhancement algorithm, where the DNN is trained to produce two source estimates that can be linearly filtered to best *explain* (i.e., reconstruct) the close-talk and far-field mixtures. In this regard, the resulting enhancement system needs to deal with three tricky issues.

First, the source estimates could be permuted randomly. That is, they could respectively correspond to speech and noise, or the opposite, since the two estimates and their linearly-filtered results are only constrained to sum up to the mixtures.

Second, the source estimates could suffer from frequency permutation [71], a common problem that needs to be dealt with in many frequency-domain unsupervised separation algorithms such as independent vector analysis, spatial clustering, and UNSSOR [35]. Since FCP is performed in each frequency independently from the others, even though speech and noise sources are accurately separated in each frequency, the separation results of each source at different frequencies are not guaranteed to be grouped into the same output spectrogram.

Third, since, in realistic cases, the noise component  $V$  usually consists of an unknown number of directional and diffuse sources, in unsupervised separation the model would lack an idea to produce one estimate exactly corresponding to target speech and the other exactly corresponding to all the noise sources combined. In other words, sources are ambiguous to the model. It is possible that, even if one estimate contains the target speech plus some noise sources and the other estimate absorbs the rest noise sources, the mixture-constraint loss can still be very low. The fundamental causes of this problem are that, in unsupervised setups, (a) the model lacks an exact concept about what the target source should be like; and (b) the hypothesized number sources (in this paper, 2) is not guaranteed to match the actual number of sources (i.e., speech source plus an unknown number of noise sources) in every training mixture.

These issues do not exist in supervised approaches, as the oracle simulated speech and noise signals used in supervised approaches can penalize the DNN estimates to naturally avoid source and frequency permutation, and resolve source ambiguity. This motivates us to combine M2M training with supervised learning, leading to SuperM2M, which is described next.

## 5. SuperM2M

The previous section points out that M2M suffers from source and frequency permutation, and source ambiguity. On the other hand, although M2M training can be performed on real mixtures, there may not be many paired close-talk and far-field real-recorded mixtures available, as collecting real data is effort-consuming. In comparison, supervised models can be readily trained on massive simulated mixtures, as one can easily simulate as many mixtures as one considers sufficient. In addition, they do not suffer from source and frequency permutation, and source ambiguity.

### 5.1. Supervised and Mixture-to-Mixture Co-Learning

In this context, we propose to train the same DNN model with both M2M training and supervised learning to combine their strengths. We name the algorithm SuperM2M. See Fig. 2 for an illustration, where the supervised learning part is shown in Fig. 2(b). Notice that the DNN in M2M training is designed to directly produce target and non-target estimates. This makes M2M training capable of being easily integrated with supervised training, where the models are usually designed to directly produce target estimates.

In detail, at each training step, we sample either a mini-batch of real close-talk and far-field mixture pairs or a mini-batch of simulated far-field mixtures for DNN training. The loss on real data is  $\mathcal{L}_{\text{MC}}$  in (5), and the loss on simulated data is

$$\mathcal{L}_{\text{SIMU},q} = \mathcal{L}_{\text{Target},q} + \mathcal{L}_{\text{Non-target},q}, \quad (14)$$

$$\mathcal{L}_{\text{Target},q} = \frac{1}{\sum_{t,f} |Y_q(t,f)|} \sum_{t,f} \mathcal{G}(S_q(t,f), \hat{S}_q(t,f)), \quad (15)$$

$$\mathcal{L}_{\text{Non-target},q} = \frac{1}{\sum_{t,f} |Y_q(t,f)|} \sum_{t,f} \mathcal{G}(V_q(t,f), \hat{V}_q(t,f)), \quad (16)$$



where  $\mathcal{G}(\cdot, \cdot)$  is defined in (10),  $S_q$  and  $V_q$  are obtained through simulation, and the denominator balances the loss values with the ones in M2M training.

## 5.2. Necessity of Close-Talk Mixtures

So far, we hypothesize that, during training, a paired close-talk mixture is always available for far-field mixtures. It is leveraged as a weak supervision for training by optimizing a mixture-constraint loss (i.e.,  $\mathcal{L}_{MC,0}$  in (8)) defined on it.

When close-talk mixtures are not available, we find that we can still train enhancement models successfully via SuperM2M, where, in the M2M part, the DNN is trained to only recover far-field mixtures, meaning that M2M training is unsupervised.<sup>3</sup> This is a desirable property, as this means that we only need a set of real-recorded far-field multi-channel mixtures (which are easier to record than paired far-field and close-talk mixtures), and together with a set of simulated mixtures, we can train an enhancement system via SuperM2M, which could generalize better to real mixtures than purely-supervised models trained only on the simulated mixtures.

## 6. Experimental Setup

Our main goal is to show that SuperM2M can generalize better to real data than purely supervised models trained on simulated data. We follow the robust ASR pipeline in Fig. 3 for evaluation, not using any joint frontend-backend training.

We do not use  $\hat{S}_q$  to derive linear beamforming results for ASR [1, 33, 43], although this has been extremely popular, as we would like to validate whether the enhanced speech  $\hat{S}_q$  itself is close to target speech and whether  $\hat{S}_q$  itself can yield better ASR performance. We do not jointly train enhancement models with ASR models, as this requires knowledge of ASR models and would not accurately reflect the accuracy of  $\hat{S}_q$  itself. We aim at building enhancement models that can produce enhanced speech with low distortion and high reduction to non-target signals. This way, the enhancement models could improve the robustness of many subsequent applications, not just limited to ASR.

In a nutshell, our main goal is to show, through SuperM2M, whether  $\hat{S}_q$  itself would be better on real test data. We validate SuperM2M on CHiME-4 [42], a dataset consisting of simulated mixtures and real-recorded close-talk and far-field mixture pairs. To further show the effectiveness and potential of SuperM2M, a minor goal is to show whether SuperM2M can lead to state-of-the-art ASR performance on CHiME-4.

The rest of this section describes the CHiME-4 dataset, miscellaneous system configurations, comparison systems, evaluation metrics, and several tricks to improve robust ASR performance.

<sup>3</sup>When close-talk mixtures are not available, M2M [40] regresses to UNSSOR [35]. In our paper, we prefer to still call our algorithms SuperM2M, rather than SuperUNSSOR, just to avoid creating too many new names.

Table 2: Number of utterances in CHiME-4 (all are six-channel)

Type	Training Set	Validation Set	Test Set
SIMU	7,138 (~15.1 h)	1,640 (~2.9 h) (410 in each environ.)	1,320 (~2.3 h) (330 in each environ.)
REAL	1,600 (~2.9 h)	1,640 (~2.7 h) (410 in each environ.)	1,320 (~2.2 h) (330 in each environ.)

### 6.1. CHiME-4 Dataset

CHiME-4 [42] is a major corpus for evaluating robust ASR and speech enhancement algorithms. It is recorded by using a tablet mounted with 6 microphones, with the second microphone on the rear and the others facing front. The signals are recorded in four representative environments (including cafeteria, buses, pedestrian areas, and streets), where reverberation and directional, diffuse, transient and non-stationary noises naturally exist. During data collection, the target speaker hand-holds the tablet in a designated environment, and reads text prompts shown on the screen of the tablet. The target speaker wears a close-talk microphone so that the close-talk mixture can be recorded at the same time along with far-field mixtures recorded by the microphones on the tablet. The number of simulated and real-recorded utterances is listed in Table 2.

In the real data of CHiME-4, we observe synchronization errors between the close-talk microphone and far-field microphone array. Other issues, such as microphone failures, signal clipping, speaker and array movement, and diverse gain levels even if microphones are placed close to each other, happen frequently. In real-world products, these are typical problems, which increase the difficulties of speech enhancement and ASR. They need to be robustly dealt with by frontend enhancement systems.

Depending on the number of microphones that can be used for recognition, there are three official ASR tasks in CHiME-4, including 1-, 2- and 6-channel tasks. In the 1-channel task, only one of the front microphones can be used for testing; in the 2-channel task, only two of the front microphones can be used; and in the 6-channel task, all the six microphones can be used. For the 1- and 2-channel tasks, the microphones that can be used for ASR for each utterance are selected by the challenge organizers to avoid microphone failures. The selected microphones can vary from utterance to utterance.

### 6.2. Evaluation Setup - Robust ASR

We check whether SuperM2M can improve ASR performance by feeding its enhanced speech to ASR models for decoding, following the pipeline in Fig. 3. We consider two ASR models. The first one is Whisper Large v2<sup>4</sup> [73], pre-trained on massive data. We use its text normalizer to normalize hypothesis and reference text before computing WER. The second one is trained on the official CHiME-4 mixtures plus the clean signals in WSJ0 by using the public recipe [53]<sup>5</sup> in ESPnet. It is an

<sup>4</sup><https://huggingface.co/openai/whisper-large-v2>

<sup>5</sup>[https://github.com/espnet/espnet/blob/master/egs2/chime4/asr1/conf/tuning/train\\_asr\\_transformer\\_wavlm\\_lr1e-3\\_specaug\\_accum1\\_preenc128\\_warmup20k.yaml](https://github.com/espnet/espnet/blob/master/egs2/chime4/asr1/conf/tuning/train_asr_transformer_wavlm_lr1e-3_specaug_accum1_preenc128_warmup20k.yaml)

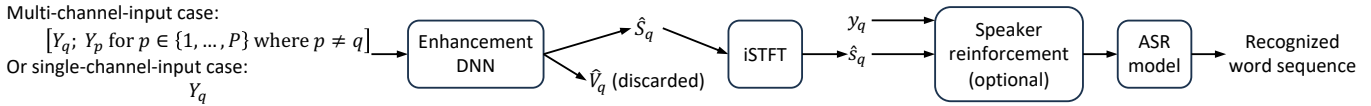


Figure 3: Robust ASR pipeline, where enhanced speech  $\hat{s}_q = \text{iSTFT}(\hat{S}_q)$  is fed to backend ASR models for recognition. No joint training is performed. An optional speaker reinforcement module [72], which adds a scaled version of the input mixture signal  $y_q$  to  $\hat{s}_q$ , can be included.

encoder-decoder transformer-based model, trained on WavLM features [74] and using a transformer language model in decoding. Note that the WERs computed by ESPnet should not be directly compared with the ones by Whisper due to different text normalization.

### 6.3. Evaluation Setup - Speech Enhancement

We evaluate the enhancement performance of SuperM2M on the simulated test data of CHiME-4. We consider 1- and 6-channel enhancement. In the 1-channel case, SuperM2M uses the fifth microphone (CH5) signal as input, and the target direct-path signal at CH5 is used as the reference for evaluation. In the 6-channel case, SuperM2M uses all the microphone signals as input to predict the target speech at CH5.

The evaluation metrics include wide-band perceptual evaluation of speech quality (WB-PESQ) [75], short-time objective intelligibility (STOI) [76], signal-to-distortion ratio (SDR) [77], and scale-invariant SDR (SISDR) [78]. They are widely-adopted metrics in speech enhancement, which can evaluate the quality, intelligibility, and accuracy of the magnitude and phase of enhanced speech.

### 6.4. Training Setup

For monaural enhancement, we train SuperM2M using all the  $(7, 138 + 1, 600) \times 6$  monaural signals. For 2-channel enhancement, at each training step we sample 2 microphones from the front microphones as input, and train the DNN to predict the target speech at the first of the selected microphones. For 6-channel enhancement, we train SuperM2M using the 7, 138 + 1, 600 six-channel signals. The DNN stacks all the six microphones as input to predict the target speech at CH5.

For simplicity, we do not filter out microphone signals with any microphone failures in the DNN input and loss. We would expect SuperM2M to learn to deal with the failures, as it can be trained on real mixtures.

### 6.5. Miscellaneous Configurations

For STFT, the window size is 32 ms, hop size 8 ms, the square root of Hann window is used as the analysis window, and the synthesis window is designed based on the analysis window to achieve perfect reconstruction.

TF-GridNet [18], which has shown strong separation performance in major benchmarks in supervised speech separation, is used as the DNN architecture. We consider two setups. Using the symbols defined in Table I of [18], the first one (denoted as TFGridNetv1) sets its hyper-parameters to  $D = 100$ ,  $B = 4$ ,  $I = 2$ ,  $J = 2$ ,  $H = 200$ ,  $L = 4$  and  $E = 2$ , and the second one (denoted as TFGridNetv2) to  $D = 128$ ,  $B = 4$ ,  $I = 1$ ,  $J = 1$ ,

$H = 200$ ,  $L = 4$  and  $E = 4$ . Please do not confuse these symbols with the ones in this paper. The models have  $\sim 6.3$  and  $\sim 5.4$  million parameters respectively. The v1 model uses around half of the computation and memory of v2, and is utilized for faster experimentation.

We train all the enhancement models on 8-second segments using a mini-batch size of 1. At each training step, if the sampled utterance is simulated, we use supervised learning, and if it is real-recorded, we use M2M training. Adam is employed for optimization. The learning rate starts from 0.001 and is halved if the validation loss is not improved in 2 epochs.

### 6.6. Comparison Systems

We consider the same DNN model trained only on the simulated data of CHiME-4 via supervised learning as the major baseline for comparison. We use exactly the same configurations as that in SuperM2M for training. We denote this baseline as **Supervised**, to differentiate it with **SuperM2M**. Since CHiME-4 is a public and popular dataset, many existing models can be used directly for comparison.

### 6.7. Tricks to Improve Robust ASR Performance

To show the effectiveness of SuperM2M, we also check whether it can lead to state-of-the-art ASR performance on CHiME-4. This subsection describes several tricks that are known to improve robust ASR performance and are commonly used in existing studies.

#### 6.7.1. SNR Augmentation for Simulated Training Mixtures

At each training step, we optionally modify the SNR of the target speech in the CHiME-4 simulated training mixture, on the fly, by  $u$  dB, with  $u$  uniformly sampled from the range  $[-10, +5]$  dB. In our experiments, we find this technique often producing slightly better enhancement and ASR, but not critical. Note that we do not change the combinations of speech and noise files to create new mixtures, and we just change the SNR of the existing mixtures in CHiME-4. No other data augmentation is used for enhancement.

#### 6.7.2. iSTFT-STFT Projection

We apply inverse STFT (iSTFT) followed by STFT operations to the DNN estimates  $\hat{S}_q$  and  $\hat{V}_q$  before loss computation, i.e.,  $\hat{S}_q := \text{STFT}(\text{iSTFT}(\hat{S}_q))$  and  $\hat{V}_q := \text{STFT}(\text{iSTFT}(\hat{V}_q))$ . See Fig. 2 for an illustration. This often yields slight improvement, as the losses now penalize the RI components and magnitudes extracted from re-synthesized signals, which are the final system output used for human hearing and downstream tasks [79, 80, 69]. Notice that, in Fig. 3, ASR features are extracted from re-synthesized signals.

Table 3: SuperM2M vs. purely-supervised models on CHiME-4  
 (#input mics: 1; ASR model: Whisper Large v2)

Row	Systems	Training data	DNN arch.	$\tilde{J}$	#mics in $\mathcal{L}_{MC}$	SNR aug.	iSTFT-STFT proj.	Spk. reinf. $\gamma$ (dB)	SIMU Test Set (CH5)				Official CHiME-4 Test Utterances			
									SISDR (dB) $\uparrow$	SDR (dB) $\uparrow$	WB-PESQ $\uparrow$	STOI $\uparrow$	Val. WER (%) $\downarrow$	REAL	SIMU	REAL
0	Mixture	-	-	-	-	-	-	-	7.5	7.5	1.27	0.870	7.43	4.96	10.97	7.69
1a	Supervised	S	TFGridNetv1	-	-	$\times$	$\times$	-	17.1	<b>17.5</b>	2.44	0.960	7.14	5.33	13.16	10.20
1b	Supervised	S	TFGridNetv2	-	-	$\checkmark$	$\checkmark$	-	17.1	<b>17.5</b>	2.44	0.961	7.58	5.19	12.44	9.03
2	Supervised	S	iNeuBe [13]	-	-	-	-	-	15.1	-	-	0.954	-	-	-	-
3	SuperM2M	S+R	TFGridNetv1	-	6	$\times$	$\times$	-	16.8	17.3	2.40	0.960	7.13	5.17	11.80	7.02
4a	SuperM2M	S+R	TFGridNetv1	1	6+1	$\times$	$\times$	-	16.8	17.4	2.38	0.961	7.10	5.05	11.87	6.93
4b	SuperM2M	S+R	TFGridNetv1	2	6+1	$\times$	$\times$	-	16.9	<b>17.5</b>	2.45	0.962	6.99	5.19	11.67	6.87
4c	SuperM2M	S+R	TFGridNetv1	3	6+1	$\times$	$\times$	-	16.6	<b>17.5</b>	2.47	0.961	7.02	4.86	12.26	6.86
4d	SuperM2M	S+R	TFGridNetv1	4	6+1	$\times$	$\times$	-	16.8	<b>17.5</b>	2.48	<b>0.963</b>	7.10	4.97	11.75	6.87
4d	SuperM2M	S+R	TFGridNetv1	5	6+1	$\times$	$\times$	-	16.9	17.4	2.36	0.959	7.34	5.29	12.23	7.51
4e	SuperM2M	S+R	TFGridNetv1	6	6+1	$\times$	$\times$	-	16.9	17.4	2.41	0.962	7.34	5.29	12.23	7.51
4f	SuperM2M	S+R	TFGridNetv1	7	6+1	$\times$	$\times$	-	<b>17.0</b>	17.4	2.42	0.961	7.23	5.02	12.19	6.90
4g	SuperM2M	S+R	TFGridNetv1	8	6+1	$\times$	$\times$	-	16.6	17.4	2.41	0.961	7.26	5.03	12.05	6.95
5	SuperM2M	S+R	TFGridNetv1 est.	6+1	$\times$	$\times$	-	16.4	17.4	<b>2.56</b>	0.962	7.01	4.87	11.69	6.51	
6a	UNSSOR [35]	R	TFGridNetv1	-	6	$\times$	$\times$	-	10.3	11.0	1.42	0.898	11.02	6.24	15.04	10.42
6b	UNSSOR [35]	S+R	TFGridNetv1	-	6	$\times$	$\times$	-	11.6	11.7	1.70	0.937	7.71	5.24	11.85	8.12
6c	M2M [40]	R	TFGridNetv1 est.	6+1	$\times$	$\times$	-	11.6	12.3	1.77	0.924	10.72	5.95	14.98	8.61	
6d	M2M [40]	S+R	TFGridNetv1 est.	6+1	$\times$	$\times$	-	10.3	10.4	1.77	0.942	7.70	5.66	11.94	8.00	
7	SuperM2M	S+R	TFGridNetv2 est.	6+1	$\checkmark$	$\checkmark$	-	16.6	17.4	2.51	<b>0.963</b>	7.05	4.78	11.34	6.02	
8a	SuperM2M	S+R	TFGridNetv2 est.	6+1	$\checkmark$	$\checkmark$	10	-	-	-	-	<b>5.90</b>	<b>4.42</b>	<b>8.80</b>	<b>5.80</b>	
8b	SuperM2M	S+R	TFGridNetv2 est.	6+1	$\checkmark$	$\checkmark$	15	-	-	-	-	6.22	4.47	9.34	5.76	
8c	SuperM2M	S+R	TFGridNetv2 est.	6+1	$\checkmark$	$\checkmark$	20	-	-	-	-	6.40	4.60	9.87	5.86	
9	Close-talk Mixture	-	-	-	-	-	-	-	-	-	-	-	3.76	-	3.91	

### 6.7.3. Run-Time Speaker Reinforcement for Robust ASR

At run time, in default we feed  $\hat{s}_q$  for ASR. Alternatively, we employ a technique named *speaker reinforcement* [72], where  $\hat{s}_q$  is re-mixed with the input mixture  $y_q$  at an energy level of  $\gamma$  dB before recognition. See Fig. 3 for an illustration. That is,  $\hat{s}_q + \eta \times y_q$ , where  $\eta \in \mathbb{R}_{>0}$  and  $\gamma = 10 \times \log_{10}(\|\hat{s}_q\|^2 / \|\eta \times y_q\|^2)$ . We find this technique usually effective for ASR, as the re-mixed input mixture can alleviate distortion to target speech.

## 7. Evaluation Results

This section reports our evaluations results on CHiME-4. Following earlier studies [35, 40], we set  $\tilde{I}$  and  $\tilde{J}$  (described in Table 1) to 20, and  $\tilde{J}$  to 1.  $\tilde{J}$  can be tuned to a value shared for all the training mixtures, or it can be estimated, on the fly, for each training mixture by using the method described in Section 4.4. Since CHiME-4 is known to contain minor reverberation, we set both  $K$  and  $\Delta$  to 0, meaning that  $\tilde{\mathbf{S}}_q(t, f)$  and  $\tilde{\mathbf{g}}_q(f)$  in (6) do not exist. All the six far-field microphones are used for computing  $\mathcal{L}_{MC}$  in (5). We emphasize that we spent minimal amount of effort on hyper-parameter tuning. Other hyper-parameter setup could lead to better performance.

### 7.1. SuperM2M vs. Purely-Supervised Models

Table 3 and 4 respectively report 1- and 6-channel enhancement performance on the fifth microphone of the CHiME-4

simulated test data, and robust ASR performance on the official CHiME-4 test utterances (by using the Whisper Large v2 model for recognition). The two tables consist of exactly the same set of experiments, and differ only in the number of input microphones to the enhancement models.

On the simulated test data, purely supervised models (in row 1a-1b) trained on the official simulated training data (denoted as **S** in the ‘‘Training data’’ column) produce large improvement over unprocessed mixtures (e.g., in row 1a of Table 3, 17.1 vs. 7.5 dB SISDR, and in 1a of Table 4, 22.2 vs. 7.5 dB SISDR), and achieve enhancement performance better than existing supervised models such as iNeuBe (based on TCN-DenseUNet) [13, 81], SpatialNet [23], USES [24] and USES2 [25] in both 1- and 6-channel cases. However, the ASR performance is much worse than directly using unprocessed mixtures for ASR, especially in multi-channel cases (e.g., in row 1a and 0 of Table 3, 10.20% vs. 7.69% WER on REAL test data, and in row 1a and 0 of Table 4, 53.23% vs. 7.69% WER on REAL test data). This degradation has been widely observed by existing studies [33, 43], largely due to the mismatches between simulated training and real-recorded test conditions, and the speech distortion incurred by enhancement.

In row 7 of Table 3 and 4, we respectively show the results of our best performing SuperM2M models (without employing the speaker reinforcement technique described in Section 6.7.3) for 1- and 6-channel cases. By training on the official simulated and real data combined (denoted as **S+R**), SuperM2M obtains

Table 4: SuperM2M vs. purely-supervised models on CHiME-4  
 (#input mics: 6; ASR model: Whisper Large v2)

Row	Systems	Training data	DNN arch.	$\tilde{J}$	#mics in $\mathcal{L}_{MC}$	SNR aug.	iTFT- STFT proj.?	Spk. reinf. $\gamma$ (dB)	SIMU Test Set (CH5)				Official CHiME-4 Test Utterances			
									SISDR (dB)↑	SDR (dB)↑	WB-PESQ↑	STOI↑	Val. SIMU	WER (%)↓	REAL	Test WER (%)↓
0	Mixture	-	-	-	-	-	-	-	7.5	7.5	1.27	0.870	7.43	4.96	10.97	7.69
1a	Supervised	S	TFGridNetv1	-	-	✗	✗	-	22.2	22.6	3.08	0.984	3.55	28.90	3.93	53.23
1b	Supervised	S	TFGridNetv2	-	-	✓	✓	-	<b>22.8</b>	<b>23.2</b>	<b>3.36</b>	<b>0.988</b>	3.43	58.15	3.79	79.08
2a	Supervised	S	iNeuBe [13]	-	-	-	-	-	22.0	22.4	-	0.986	-	-	-	-
2b	Supervised	S	SpatialNet [23]	-	-	-	-	-	22.1	22.3	2.88	0.983	-	-	-	-
2c	Supervised	S	USES [24]	-	-	-	-	-	-	20.6	3.16	0.983	-	-	4.20	78.10
2d	Supervised	S	USES2 [25]	-	-	-	-	-	-	18.8	2.94	0.979	-	-	4.60	12.10
3	SuperM2M	S+R	TFGridNetv1	-	6	✗	✗	-	22.3	22.6	3.12	0.984	3.52	3.93	3.93	4.46
4a	SuperM2M	S+R	TFGridNetv1	1	6+1	✗	✗	-	22.3	22.5	3.06	0.984	3.57	3.89	3.97	4.04
4b	SuperM2M	S+R	TFGridNetv1	2	6+1	✗	✗	-	22.2	22.6	3.11	0.984	3.51	3.84	4.12	4.16
4c	SuperM2M	S+R	TFGridNetv1	3	6+1	✗	✗	-	22.2	22.5	3.07	0.984	3.56	3.88	4.05	4.09
4d	SuperM2M	S+R	TFGridNetv1	4	6+1	✗	✗	-	22.4	22.7	3.11	0.985	3.48	3.97	3.98	4.07
4d	SuperM2M	S+R	TFGridNetv1	5	6+1	✗	✗	-	22.3	22.6	3.07	0.985	3.52	3.97	4.05	4.16
4e	SuperM2M	S+R	TFGridNetv1	6	6+1	✗	✗	-	22.3	22.7	3.10	0.985	3.61	3.94	3.98	4.21
4f	SuperM2M	S+R	TFGridNetv1	7	6+1	✗	✗	-	22.2	22.5	3.10	0.984	3.53	3.99	4.01	4.24
4g	SuperM2M	S+R	TFGridNetv1	8	6+1	✗	✗	-	22.4	22.7	3.14	0.985	3.51	3.93	3.97	4.19
5	SuperM2M	S+R	TFGridNetv1	est.	6+1	✗	✗	-	22.3	22.6	3.07	0.985	3.59	3.92	4.08	<b>3.97</b>
6a	UNSSOR [35]	R	TFGridNetv1	-	6	✗	✗	-	7.7	8.1	1.30	0.870	4.82	4.16	6.20	4.84
6b	UNSSOR [35]	S+R	TFGridNetv1	-	6	✗	✗	-	4.5	4.6	1.32	0.881	4.81	4.14	5.42	4.88
6c	M2M [40]	R	TFGridNetv1	est.	6+1	✗	✗	-	9.8	10.3	1.50	0.902	4.94	3.95	6.76	4.32
6d	M2M [40]	S+R	TFGridNetv1	est.	6+1	✗	✗	-	4.5	4.6	1.33	0.882	4.63	3.95	5.38	4.32
7	SuperM2M	S+R	TFGridNetv2	est.	6+1	✓	✓	-	<b>22.8</b>	<b>23.2</b>	3.22	0.987	<b>3.38</b>	<b>3.81</b>	3.77	4.04
8a	SuperM2M	S+R	TFGridNetv2	est.	6+1	✓	✓	10	-	-	-	-	3.61	3.85	3.84	4.24
8b	SuperM2M	S+R	TFGridNetv2	est.	6+1	✓	✓	15	-	-	-	-	3.59	3.87	<b>3.74</b>	4.11
8c	SuperM2M	S+R	TFGridNetv2	est.	6+1	✓	✓	20	-	-	-	-	3.54	3.86	<b>3.74</b>	4.10
9	Close-talk Mixture	-	-	-	-	-	-	-	-	-	-	-	-	3.76	-	3.91

clearly better ASR results on the real test data than the purely-supervised models (in row 1a-1b) and unprocessed mixtures (in row 0), and the enhancement performance on the simulated test data remains strong. These results indicate that SuperM2M can effectively learn from real data, has better generalizability to real data, and can perform enhancement with low distortion to target speech and high reduction to non-target signals.

Next, we present some ablations results of SuperM2M.

### 7.2. Effects of Including Loss on Close-Talk Mixture in $\mathcal{L}_{MC}$

First, we report the results of not including close-talk microphone in the loss function. That is, in (5) we do not include the third term,  $\mathcal{L}_{MC,0}$ , when training SuperM2M. We observe clear improvement in ASR performance on the real test data over the purely-supervised model in row 1a (i.e., 7.02% vs. 10.20% in Table 3 and 4.46% vs. 53.23% in Table 4), indicating that close-talk mixtures are not must-have for our system.

Next, we include close-talk mixtures for training. In row 4a-4g, the number of future taps for the close-talk microphone,  $\tilde{J}$ , is tuned to a value shared by all the training utterances. We enumerate  $\tilde{J}$  from 1 all the way up to 8. In row 5, we instead estimate  $\tilde{J}$ , on the fly, for each training mixture during training, using the technique described in Section 4.4. Compared with row 4a-4g, row 5 obtains better ASR performance on the real test data, indicating the effectiveness of the proposed way of estimating  $\tilde{J}$ .

In both Table 3 and 4, comparing row 5 and 3, we observe that including close-talk mixtures for training SuperM2M produces better ASR performance on the real data of CHiME-4 (e.g., 6.51% vs. 7.02% in Table 3 and 3.97% vs. 4.46% in Table 4).

### 7.3. SuperM2M vs. UNSSOR and M2M

In row 6a-6d of Table 3 and 4, we respectively report the results of UNSSOR [35] and M2M [40]. UNSSOR is trained in an unsupervised way directly on far-field mixtures by using the  $\mathcal{L}_{MC}$  loss in (5) but without including the third term  $\mathcal{L}_{MC,0}$  (i.e., the loss on close-talk mixture). M2M is the same as SuperM2M but without the supervised learning branch. We can train UNSSOR and M2M on the real data alone (denoted as **R**), or on the simulated and real data combined (i.e., S+R) considering that SuperM2M is trained on S+R. When M2M is trained on S+R, the loss function on the simulated data does not include the loss on close-talk mixture, since CHiME-4 does not provide simulated close-talk mixtures.

Since the source estimates produced by UNSSOR and M2M could suffer from frequency permutation, we employ an existing algorithm [82, 83]<sup>6</sup> for frequency alignment. The algorithm exploits inter-frequency correlation of estimated source

<sup>6</sup>See [https://github.com/fgnt/pb\\_bss/blob/master/pb\\_bss/permutation\\_alignment.py](https://github.com/fgnt/pb_bss/blob/master/pb_bss/permutation_alignment.py)

Table 5: SuperM2M vs. USES [24] and USES2 [25] on CHiME-4  
(ASR model: Whisper Large v2)

Row	Cross reference	System	Training data	Task	SIMU Test (CH5)				CH5 of CHiME-4 Test Utterances			
					SISDR (dB)↑	SDR (dB)↑	WB-PESQ↑	STOI↑	Val. WER (%)↓		Test WER (%)↓	
									SIMU	REAL	SIMU	REAL
0	-	Mixture	-	1-channel	7.5	7.5	1.27	0.870	5.49	5.09	5.82	6.69
1a	-	USES [24]	S	1-channel	-	-	-	-	-	-	-	11.00
1b	-	USES [24]	S+extra	1-channel	-	-	-	-	-	-	-	7.10
2	7 of Table 3	SuperM2M	S+R	1-channel	16.6	17.4	2.51	0.963	5.37	4.84	6.14	5.73
3a	-	USES [24]	S	6-channel	-	20.6	3.16	0.983	-	-	4.20	78.10
3b	-	USES [24]	S+extra	6-channel	-	19.1	2.95	0.979	-	-	4.10	85.90
3c	-	USES2 [25]	S	6-channel	-	18.8	2.94	0.979	-	-	4.60	12.10
3d	-	USES2 [25]	S+extra	6-channel	-	-	-	-	-	-	-	10.30
4	7 of Table 4	SuperM2M	S+R	6-channel	22.8	23.2	3.22	0.987	3.38	3.81	3.77	4.04

Notes: (a) The “extra” in “SIMU+extra” means extra ~230 hours of simulated training data (see [24, 25] for details).

(b) The “cross reference” entry means that the other setups are the same as the ones in the referred row.

posteriors, and we compute the source posteriors based on the DNN estimates  $\hat{S}_q$  and  $\hat{V}_q$  respectively via  $|\hat{S}_q|/(|\hat{S}_q|+|\hat{V}_q|)$  and  $|\hat{V}_q|/(|\hat{S}_q|+|\hat{V}_q|)$ . In addition, since the source estimates of UNSSOR and M2M exhibit source permutation, for each evaluation metric we compute a score for each estimate and select the better score.

Comparing row 6a-6d and 5, we can see that SuperM2M obtains much better performance than UNSSOR and M2M, suggesting the effectiveness of the proposed co-learning mechanism. The low performance of M2M and UNSSOR is possibly because the noise in CHiME-4 typically consists of an unknown number of diffuse and directional sources. In this case, unsupervised algorithms with two hypothesized directional sources tend to get confused about which source should be the target speech source. This problem is naturally avoided by the supervised learning mechanism in SuperM2M, which models noise sources as a single, combined source.

#### 7.4. Miscellaneous Results

In row 7 of Table 3 and 4, we switch TF-GridNet from v1 to v2, perform iSTFT-STFT projection, and apply SNR augmentation. From row 5 to 7, although the ASR performance on the real test data gets better in Table 3 but worse in Table 4, in both tables better ASR performance is observed on the real validation set. We therefore use the system in row 7 as our default system for the rest experiments of this paper.

#### 7.5. SuperM2M vs. Purely Large-Scale Supervised Training

Table 5 compares SuperM2M with a representative line of research (USES [24] and USES2 [25]), which trains enhancement models in a purely-supervised way on a much larger-scale simulated data of ~245 hours, which is ~14 times the size of the CHiME-4 SIMU+REAL data (i.e., 245/(15.1 + 2.9)).

USES and USES2 have shown that, by increasing the diversity of simulated training mixtures to cover as many conditions (that could happen in real data) as possible, better enhancement

can be achieved on real data. However, on CHiME-4, compared with using unprocessed mixtures directly for recognition, they do not obtain better ASR performance, likely because the simulated training data is not representative of the real data in CHiME-4.

In comparison, SuperM2M, although trained only on the official small-scale CHiME-4 simulated and real mixtures, obtains much better ASR performance on the real data of CHiME-4 in both single- and multi-channel cases than USES, USES2, and the unprocessed mixtures. This comparison does not suggest that purely supervised learning on large-scale simulated data is a bad idea, as it can offer an easy and feasible way for training DNNs to model speech patterns for enhancement, and building upon this strength, SuperM2M can very likely produce even better enhancement on real data. Rather, it sounds an alarm that purely large-scale supervised learning on simulated data has a fundamental limitation incurred by using the current simulation techniques, which usually cannot simulate mixtures in a sufficiently realistic way. In addition, it suggests the benefits of co-training the DNN on real data via M2M. This way, the DNN, during training, can see and learn from the signal characteristics of real-recorded data, and could hence generalize better to real-recorded data.

#### 7.6. Breaking Out to New Highs on CHiME-4 ASR Tasks

Table 6 reports the ASR performance of SuperM2M based on the official ASR setup of CHiME-4, using the ASR model proposed in [53] and still following the evaluation pipeline in Fig. 3. Comparing row 0b with 0a, we observe that we have successfully reproduced the ASR system proposed in [53].

SuperM2M, despite not jointly trained with the ASR model, achieves a new state-of-the-art on the REAL test set in each of the 1-, 2- and 6-channel tasks, significantly outperforming the previous best obtained by IRIS [53] and MultiIRIS [84] (e.g., in the 1-channel case 3.04% vs. 3.92% WER in 2a and 1b, in the 2-channel case 1.94% vs. 2.65% WER in 4a and 3b, and in the 6-channel case 1.61% vs. 1.77% WER in 6a

Table 6: ASR results in official CHiME-4 setup  
(ASR model: WavLM features + encoder-decoder model [53] in ESPnet)

Row	Cross reference	Systems	Frontend	Joint training	Input #mics	Spk. reinf. $\gamma$ (dB)	Official CHiME-4 Test Utterances			
							Val. WER (%)↓		Test WER (%)↓	
						SIMU	REAL	SIMU	REAL	
0a	-	Mixture [53]	-	-	1	-	5.93	4.03	8.25	4.47
0b	-	Mixture (reproduced)	-	-	1	-	5.93	4.07	8.29	4.47
1a	-	IRIS [53]	Conv-TasNet	✗	1	-	5.96	4.37	13.52	12.11
1b	-	IRIS [53]	Conv-TasNet	✓	1	-	3.16	2.03	6.12	3.92
2a	7 of Table 3	SuperM2M	TFGridNetv2	✗	1	-	3.39	1.84	6.57	3.04
2b	7 of Table 3	SuperM2M	TFGridNetv2	✗	1	10	<b>2.40</b>	<b>1.64</b>	<b>4.54</b>	<b>2.40</b>
3a	-	MultiIRIS [84]	Neural WPD	✗	2	-	2.28	2.06	2.30	3.63
3b	-	MultiIRIS [84]	Neural WPD	✓	2	-	2.04	1.66	2.04	2.65
4a	7 of Table 4	SuperM2M	TFGridNetv2	✗	2	-	1.50	1.40	2.08	1.94
4b	7 of Table 4	SuperM2M	TFGridNetv2	✗	2	10	<b>1.28</b>	<b>1.33</b>	<b>1.88</b>	<b>1.84</b>
5a	-	MultiIRIS [84]	Neural WPD	✗	6	-	1.19	1.32	1.29	1.85
5b	-	MultiIRIS [84]	Neural WPD	✓	6	-	1.22	1.33	<b>1.24</b>	1.77
6a	7 of Table 4	SuperM2M	TFGridNetv2	✗	6	-	<b>0.83</b>	1.26	1.37	1.61
6b	7 of Table 4	SuperM2M	TFGridNetv2	✗	6	10	<b>0.83</b>	<b>1.23</b>	1.37	<b>1.58</b>
7	-	Close-talk Mixture	-	-	-	-	-	1.14	-	1.49

Notes: The best scores are highlighted in bold in the 1- and 6-channel cases separately.

and 5b). IRIS jointly trains a Conv-TasNet based monaural enhancement model, a WavLM based ASR feature extractor, and an encoder-decoder transformer based ASR model. MultiIRIS, building upon IRIS, replaces the Conv-TasNet module with a DNN based weighted power minimization distortionless response (WPD) beamformer. From row 1a vs. 1b, 3a vs. 3b, and 5a vs. 5b, we observe that, without joint training, IRIS and MultiIRIS often obtain clearly worse ASR performance, especially in the 1- and 2-channel cases. These results further indicate the effectiveness and potential of SuperM2M on real data, as it decouples enhancement and ASR and does not employ joint training.

### 7.7. Effects of Speaker Reinforcement

In row 8a-8c of Table 3 and 4, where the Whisper ASR model is used for recognition, we apply speaker reinforcement with the energy level  $\gamma$  between the enhancement output and input mixture tuned based on the set of {10, 15, 20} dB. Better ASR performance is observed in the 1-channel case but not in the 6-channel case, possibly because the enhanced speech is already reliable in the 6-channel case, rendering speaker reinforcement not necessary.

In Table 6, where the ASR system proposed in [53] is used for recognition, applying speaker reinforcement in row 2b, 4b and 6b respectively outperforms 2a, 4a and 6a, pushing down the WER on the real test set to 2.40%, 1.84% and 1.58%.

### 7.8. Comparison with Using Close-Talk Mixtures for ASR

In row 7 of Table 6 and row 9 of Table 4 and 3, we provide the ASR results of using close-talk mixtures for decoding. We observe that our proposed 6-channel system obtains ASR

results comparable to using close-talk mixtures for decoding. This further indicates the effectiveness of SuperM2M and our robust ASR system.

## 8. Conclusion

We have proposed to adapt M2M training for neural speech enhancement, where the models can be trained on real-recorded far-field mixtures in an unsupervised way, and on real-recorded close-talk and far-field mixture pairs in a weakly-supervised way. To improve M2M training, we have proposed SuperM2M, a novel co-learning algorithm that trains neural speech enhancement models by alternating between supervised training on simulated data and M2M training on real data. Evaluation results on the challenging CHiME-4 benchmark show the effectiveness of SuperM2M for speech enhancement and robust ASR. Future research will modify and evaluate SuperM2M on conversational speech separation and recognition.

Our study, we think, provides illuminating findings towards improving the generalizability of modern neural speech enhancement models to real-recorded data, since it, for the first time since the introduction of the challenging and representative CHiME-4 benchmark nearly a decade ago, shows that, on the real mixtures of CHiME-4, feeding in the immediate outputs of neural speech enhancement models for ASR decoding can produce remarkable improvement over feeding in unprocessed mixtures and neural beamforming results, breaking out to new highs in ASR performance even though joint frontend-backend training is not employed and even if the ASR backend, which leverages strong self-supervised learning representations, is a very strong one. This success is realized by SuperM2M, which

trains enhancement models not only on simulated data but also on real data, and through our accumulative efforts on complex spectral mapping [13, 14, 15], loss functions dealing with implicit magnitude-phase compensation [69], FCP [68, 70], TF-GridNet [18], UNSSOR [35], USDnet [58], and M2M [40], which have firmly built up the foundation of SuperM2M.

We point out that nearly all the current supervised neural speech enhancement algorithms can be seamlessly integrated with SuperM2M to improve their generalization abilities, by including real-recorded close-talk and far-field mixture pairs, or far-field mixtures alone if close-talk mixtures are unavailable, for M2M training. This indicates that SuperM2M can ride on the development of large-scale supervised neural speech enhancement models trained on simulated data, and has strong potential to grow into a representative algorithm for training speech enhancement models directly on real-recorded data.

In closing, we would like to highlight the learning-based methodology for solving blind deconvolution problems, which has been developed along our line of research on FCP [68, 70], UNSSOR [35], M2M [40], and SuperM2M. By training DNNs in an un-, weakly- or semi-supervised way to estimate sources, filter estimation becomes differentiable so that the DNNs can be trained to optimize mixture-constraint losses to realize separation. Based on the challenging real-recorded mixtures in CHiME-4 and through the integration with supervised learning, this paper, for the first time, has demonstrated that this methodology is effective for real-recorded data, and is also effective at neural speech enhancement. Considering that blind deconvolution broadly exists in many application domains, we expect the methodology to be also effective in similar applications and generate broader impact beyond speech enhancement.

## 9. Acknowledgments

We would like to thank Dr. Xuankai Chang at Carnegie Mellon University for constructive discussions on robust ASR.

## References

- [1] D. Wang, J. Chen, Supervised Speech Separation Based on Deep Learning: An Overview, *IEEE/ACM Trans. Audio, Speech, Lang. Process.* 26 (10) (2018) 1702–1726.
- [2] J. Chen, Y. Wang, S. E. Yoho, D. Wang, E. W. Healy, Large-Scale Training to Increase Speech Intelligibility for Hearing-Impaired Listeners in Novel Noises, *J. Acoust. Soc. Am.* 139 (5) (2016) 2604–2612.
- [3] A. Ephrat, I. Mosseri, O. Lang, T. Dekel, K. Wilson, A. Hassidim, W. T. Freeman, M. Rubinstein, Looking to Listen at the Cocktail Party: A Speaker-Independent Audio-Visual Model for Speech Separation, *ACM Trans. on Graphics* 37 (4) (2018).
- [4] Y. Luo, N. Mesgarani, Conv-TasNet: Surpassing Ideal Time-Frequency Magnitude Masking for Speech Separation, *IEEE/ACM Trans. Audio, Speech, Lang. Process.* 27 (2019) 1256–1266.
- [5] Y. Luo, Z. Chen, T. Yoshioka, Dual-Path RNN: Efficient Long Sequence Modeling for Time-Domain Single-Channel Speech Separation, in: *ICASSP*, 2020, pp. 46–50.
- [6] K. Zmolikova, M. Delcroix, T. Ochiai, K. Kinoshita, J. Cernocky, D. Yu, Neural Target Speech Extraction: An overview, *IEEE Signal Process. Mag.* 40 (3) (2023) 8–29.
- [7] I. Kavalero, S. Wisdom, H. Erdogan, B. Patton, K. Wilson, J. Le Roux, J. R. Hershey, Universal Sound Separation, in: *WASPAA*, 2019, pp. 175–179.
- [8] E. Nachmani, Y. Adi, L. Wolf, Voice Separation with An Unknown Number of Multiple Speakers, in: *ICML*, 2020, pp. 7121–7132.
- [9] N. Zeghidour, D. Grangier, Wavesplit: End-to-End Speech Separation by Speaker Clustering, *IEEE/ACM Trans. Audio, Speech, Lang. Process.* 29 (2021) 2840–2849.
- [10] Z. Chen, T. Yoshioka, L. Lu, T. Zhou, Z. Meng, Y. Luo, J. Wu, X. Xiao, J. Li, Continuous Speech Separation: Dataset and Analysis, in: *ICASSP*, 2020, pp. 7284–7288.
- [11] C. Xu, W. Rao, E. S. Chng, H. Li, SpEx: Multi-Scale Time Domain Speaker Extraction Network, *IEEE/ACM Trans. Audio, Speech, Lang. Process.* 28 (2020) 1370–1384.
- [12] Z.-Q. Wang, D. Wang, Deep Learning Based Target Cancellation for Speech Dereverberation, *IEEE/ACM Trans. Audio, Speech, Lang. Process.* 28 (2020) 941–950.
- [13] Z.-Q. Wang, P. Wang, D. Wang, Complex Spectral Mapping for Single- and Multi-Channel Speech Enhancement and Robust ASR, *IEEE/ACM Trans. Audio, Speech, Lang. Process.* 28 (2020) 1778–1787.
- [14] Z.-Q. Wang, P. Wang, D. Wang, Multi-Microphone Complex Spectral Mapping for Utterance-Wise and Continuous Speech Separation, *IEEE/ACM Trans. Audio, Speech, Lang. Process.* 29 (2021) 2001–2014.
- [15] K. Tan, Z.-Q. Wang, D. Wang, Neural Spectrospatial Filtering, *IEEE/ACM Trans. Audio, Speech, Lang. Process.* 30 (2022) 605–621.
- [16] K. Tesch, T. Gerkmann, Nonlinear Spatial Filtering in Multichannel Speech Enhancement, *IEEE/ACM Trans. Audio, Speech, Lang. Process.* 29 (2021) 1795–1805.
- [17] Z. Zhang, Y. Xu, M. Yu, S. X. Zhang, L. Chen, D. S. Williamson, D. Yu, Multi-Channel Multi-Frame ADL-MVDR for Target Speech Separation, *IEEE/ACM Trans. Audio, Speech, Lang. Process.* 29 (2021) 3526–3540.
- [18] Z.-Q. Wang, S. Cornell, S. Choi, Y. Lee, et al., TF-GridNet: Integrating Full- and Sub-Band Modeling for Speech Separation, *IEEE/ACM Trans. Audio, Speech, Lang. Process.* 31 (2023) 3221–3236.
- [19] S. R. Chetupalli, E. A. Habets, Speaker Counting and Separation From Single-Channel Noisy Mixtures, *IEEE/ACM Trans. Audio, Speech, Lang. Process.* 31 (2023) 1681–1692.
- [20] C. Zheng, H. Zhang, W. Liu, X. Luo, A. Li, et al., Sixty Years of Frequency-Domain Monaural Speech Enhancement: From Traditional to Deep Learning Methods, *Trends in Hearing* 27 (2023).
- [21] K. Saijo, W. Zhang, Z.-Q. Wang, S. Watanabe, T. Kobayashi, et al., A Single Speech Enhancement Model Unifying Dereverberation, Denoising, Speaker Counting, Separation, and Extraction, in: *ASRU*, 2023.
- [22] J. Pons, X. Liu, S. Pascual, J. Serra, GASS: Generalizing Audio Source Separation with Large-Scale Data, in: *ICASSP*, 2024.
- [23] C. Quan, X. Li, SpatialNet: Extensively Learning Spatial Information for Multichannel Joint Speech Separation, Denoising and Dereverberation, *IEEE/ACM Trans. Audio, Speech, Lang. Process.* 32 (2024) 1310–1323.
- [24] W. Zhang, K. Saijo, Z.-Q. Wang, S. Watanabe, et al., Toward Universal Speech Enhancement for Diverse Input Conditions, in: *ASRU*, 2023.
- [25] W. Zhang, J.-w. Jung, S. Watanabe, Y. Qian, Improving Design of Input Condition Invariant Speech Enhancement, in: *ICASSP*, 2024.
- [26] A. Pandey, D. Wang, On Cross-Corpus Generalization of Deep Learning Based Speech Enhancement, *IEEE/ACM Trans. Audio, Speech, Lang. Process.* 28 (2020) 2489–2499.
- [27] W. Zhang, J. Shi, C. Li, S. Watanabe, Y. Qian, Closing The Gap Between Time-Domain Multi-Channel Speech Enhancement on Real and Simulation Conditions, in: *WASPAA*, 2021, pp. 146–150.
- [28] E. Tzinis, Y. Adi, V. K. Ithapu, B. Xu, P. Smaragdis, A. Kumar, RemixIT: Continual Self-Training of Speech Enhancement Models via Bootstrapped Remixing, *IEEE J. of Sel. Topics in Signal Process.* 16 (6) (2022) 1329–1341.
- [29] E. Tzinis, S. Wisdom, T. Remez, J. R. Hershey, AudioScopeV2: Audio-Visual Attention Architectures for Calibrated Open-Domain On-Screen Sound Separation, in: *ECCV*, 2022, pp. 368–385.
- [30] T. J. Cox, J. Barker, W. Bailey, S. Graetzer, M. A. Akeroyd, J. F. Culling, G. Naylor, Overview of The 2023 ICASSP SP Clarity Challenge: Speech Enhancement For Hearing Aids, in: *ICASSP*, 2023.
- [31] S. Leglaive, L. Borne, E. Tzinis, M. Sadeghi, M. Fraticelli, S. Wisdom, M. Pariente, et al., The CHiME-7 UDASE Task: Unsupervised Domain Adaptation for Conversational Speech Enhancement, in: *CHiME*, 2023.
- [32] S. Cornell, M. Wiesner, S. Watanabe, D. Raj, X. Chang, P. Garcia, et al., The CHiME-7 DASR Challenge: Distant Meeting Transcription with Multiple Devices in Diverse Scenarios, in: *CHiME*, 2023.

- [33] R. Haeb-Umbach, S. Watanabe, T. Nakatani, M. Bacchiani, B. Hoffmeister, M. L. Seltzer, et al., Speech Processing for Digital Home Assistants: Combining Signal Processing with Deep-Learning Techniques, *IEEE Signal Process. Mag.* 36 (6) (2019) 111–124.
- [34] Y. Yang, A. Pandey, D. Wang, Towards Decoupling Frontend Enhancement and Backend Recognition in Monaural Robust ASR, arXiv preprint arXiv:2403.06387 (2024).
- [35] Z.-Q. Wang, S. Watanabe, UNSSOR: Unsupervised Neural Speech Separation by Leveraging Over-determined Training Mixtures, in: *NeurIPS*, 2023, pp. 34021–34042.
- [36] J. Barker, S. Watanabe, E. Vincent, J. Trmal, The Fifth 'CHiME' Speech Separation and Recognition Challenge: Dataset, Task and Baselines, in: *Interspeech*, 2018, pp. 1561–1565.
- [37] J. Carletta, et al., The AMI Meeting Corpus: A Pre-Announcement, in: *Machine Learning for Multimodal Interact.*, Vol. 3869, 2006, pp. 28–39.
- [38] F. Yu, et al., M2MeT: The ICASSP 2022 Multi-Channel Multi-Party Meeting Transcription Challenge, in: *ICASSP*, 2022, pp. 6167–6171.
- [39] S. Wu, C. Wang, H. Chen, Y. Dai, C. Zhang, R. Wang, H. Lan, et al., The Multimodal Information Based Speech Processing (MISP) 2023 Challenge: Audio-Visual Target Speaker Extraction, in: *ICASSP*, 2024.
- [40] Z.-Q. Wang, Mixture to Mixture: Leveraging Close-talk Mixtures as Weak-supervision for Speech Separation, arXiv preprint arXiv:2402.09313 (2024).
- [41] S. Watanabe, M. Mandel, J. Barker, E. Vincent, et al., CHiME-6 Challenge: Tackling Multispeaker Speech Recognition for Unsegmented Recordings, in: arXiv preprint arXiv:2004.09249, 2020.
- [42] E. Vincent, S. Watanabe, A. A. Nugraha, J. Barker, R. Marxer, An Analysis of Environment, Microphone and Data Simulation Mismatches in Robust Speech Recognition, *Comp. Speech and Lang.* 46 (2017) 535–557.
- [43] R. Haeb-Umbach, J. Heymann, L. Drude, S. Watanabe, M. Delcroix, T. Nakatani, Far-Field Automatic Speech Recognition, *Proc. IEEE* (2020).
- [44] J. Heymann, L. Drude, A. Chinaev, R. Haeb-Umbach, BLSTM Supported GEV Beamformer Front-End for The 3rd CHiME Challenge, in: *ASRU*, 2015, pp. 444–451.
- [45] X. Zhang, Z.-Q. Wang, D. Wang, A Speech Enhancement Algorithm by Iterating Single- and Multi-Microphone Processing and Its Application to Robust ASR, in: *ICASSP*, 2017, pp. 276–280.
- [46] C. Boeddecker, J. Heitkaemper, J. Schmalenstroerer, L. Drude, J. Heymann, R. Haeb-Umbach, Front-End Processing for The CHiME-5 Dinner Party Scenario, in: *CHiME*, 2018, pp. 35–40.
- [47] A. Narayanan, D. Wang, Improving Robustness of Deep Neural Network Acoustic Models via Speech Separation and Joint Adaptive Training, *IEEE/ACM Trans. Audio, Speech, Lang. Process.* 23 (1) (2015) 92–101.
- [48] Z.-Q. Wang, D. Wang, A Joint Training Framework for Robust Automatic Speech Recognition, *IEEE/ACM Trans. Audio, Speech, Lang. Process.* 24 (4) (2016) 796–806.
- [49] J. Heymann, L. Drude, C. Boeddecker, P. Hanebrink, R. Haeb-Umbach, BEAMNET: End-To-End Training of A Beamformer-Supported Multi-Channel ASR System, in: *ICASSP*, 2017, pp. 5325–5329.
- [50] X. Chang, W. Zhang, Y. Qian, J. Le Roux, S. Watanabe, MIMO-SPEECH: End-to-End Multi-Channel Multi-Speaker Speech Recognition, in: *ASRU*, 2019, pp. 237–244.
- [51] S. Gannot, E. Vincent, S. Markovich-Golan, A. Ozerov, A Consolidated Perspective on Multi-Microphone Speech Enhancement and Source Separation, *IEEE/ACM Trans. Audio, Speech, Lang. Process.* 25 (2017) 692–730.
- [52] Y. Masuyama, X. Chang, W. Zhang, S. Cornell, Z.-Q. Wang, N. Ono, Y. Qian, S. Watanabe, Exploring The Integration of Speech Separation and Recognition with Self-Supervised Learning Representation, in: *WASPAA*, 2023, pp. 1–5.
- [53] X. Chang, T. Maekaku, Y. Fujita, S. Watanabe, End-to-End Integration of Speech Recognition, Speech Enhancement, and Self-Supervised Learning Representation, in: *Interspeech*, 2022, pp. 3819–3823.
- [54] S. Wisdom, E. Tzinis, H. Erdogan, R. J. Weiss, K. Wilson, J. R. Hershey, Unsupervised Sound Separation using Mixture Invariant Training, in: *NeurIPS*, 2020.
- [55] T. Fujimura, Y. Koizumi, K. Yatabe, R. Miyazaki, Noisy-target Training: A Training Strategy for DNN-based Speech Enhancement without Clean Speech, in: *EUSIPCO*, 2021, pp. 436–440.
- [56] Y. Bando, K. Sekiguchi, Y. Masuyama, A. A. Nugraha, M. Fontaine, K. Yoshii, Neural Full-Rank Spatial Covariance Analysis for Blind Source Separation, *IEEE Signal Process. Lett.* 28 (2021) 1670–1674.
- [57] R. Aralikatti, C. Boeddecker, G. Wichern, A. S. Subramanian, J. Le Roux, Reverberation as Supervision for Speech Separation, in: *ICASSP*, 2023.
- [58] Z.-Q. Wang, USDnet: Unsupervised Speech Dereverberation via Neural Forward Filtering, arXiv preprint arXiv:2402.00820 (2024).
- [59] A. Sivaraman, S. Wisdom, H. Erdogan, J. R. Hershey, Adapting Speech Separation To Real-World Meetings using Mixture Invariant Training, in: *ICASSP*, 2022, pp. 686–690.
- [60] C. Han, K. Wilson, S. Wisdom, J. R. Hershey, Unsupervised Multi-channel Separation and Adaptation, in: *ICASSP*, 2024, pp. 721–725.
- [61] J. Zhang, C. Zorilă, R. Doddipatla, J. Barker, On Monoaural Speech Enhancement for Automatic Recognition of Real Noisy Speech using Mixture Invariant Training, in: *Interspeech*, 2022, pp. 1056–1060.
- [62] X. Hao, C. Xu, L. Xie, Neural Speech Enhancement with Unsupervised Pre-Training and Mixture Training, *Neural Networks* 158 (2023) 216–227.
- [63] D. Stoller, S. Ewert, S. Dixon, Adversarial Semi-Supervised Audio Source Separation Applied to Singing Voice Extraction, in: *ICASSP*, 2018, pp. 2391–2395.
- [64] N. Zhang, J. Yan, Y. Zhou, Weakly Supervised Audio Source Separation via Spectrum Energy Preserved Wasserstein Learning, in: *IJCAI*, 2018, pp. 4574–4580.
- [65] F. Pishdadian, G. Wichern, J. Le Roux, Finding Strength in Weakness: Learning to Separate Sounds with Weak Supervision, in: *IEEE/ACM Trans. Audio, Speech, Lang. Process.*, Vol. 28, 2020, pp. 2386–2399.
- [66] R. Talmon, I. Cohen, S. Gannot, Relative Transfer Function Identification using Convolutional Transfer Function Approximation, *IEEE Trans. Audio, Speech, Lang. Process.* 17 (4) (2009) 546–555.
- [67] A. Levin, Y. Weiss, F. Durand, W. T. Freeman, Understanding Blind Deconvolution Algorithms, *IEEE Trans. Pattern Anal. Mach. Intell.* 33 (12) (2011) 2354–2367.
- [68] Z.-Q. Wang, G. Wichern, J. Le Roux, Convolutional Prediction for Monaural Speech Dereverberation and Noisy-Reverberant Speaker Separation, *IEEE/ACM Trans. Audio, Speech, Lang. Process.* 29 (2021) 3476–3490.
- [69] Z.-Q. Wang, G. Wichern, J. Le Roux, On The Compensation Between Magnitude and Phase in Speech Separation, *IEEE Signal Process. Lett.* 28 (2021) 2018–2022.
- [70] Z.-Q. Wang, G. Wichern, J. Le Roux, Convolutional Prediction for Reverberant Speech Separation, in: *WASPAA*, 2021, pp. 56–60.
- [71] H. Sawada, N. Ono, H. Kameoka, D. Kitamura, H. Saruwatari, A Review of Blind Source Separation Methods: Two Converging Routes to ILRMA Originating from ICA and NMF, *APSIPA Trans. on Signal and Info. Process.* 8 (2019) 1–14.
- [72] C. Zorilă, R. Doddipatla, Speaker Reinforcement using Target Source Extraction for Robust Automatic Speech Recognition, in: *ICASSP*, 2022, pp. 6297–6301.
- [73] A. Radford, J. W. Kim, T. Xu, G. Brockman, C. McLeavey, I. Sutskever, Robust Speech Recognition via Large-Scale Weak Supervision, *Proc. Mach. Learn. Res.* 202 (2023) 28492–28518.
- [74] S. Chen, C. Wang, Z. Chen, Y. Wu, S. Liu, Z. Chen, J. Li, N. Kanda, T. Yoshioka, X. Xiao, J. Wu, L. Zhou, S. Ren, et al., WavLM: Large-Scale Self-Supervised Pre-Training for Full Stack Speech Processing, in: *IEEE J. of Sel. Topics in Signal Process.*, Vol. 16, 2022, pp. 1505–1518.
- [75] A. Rix, J. Beerends, M. Hollier, A. Hekstra, Perceptual Evaluation of Speech Quality (PESQ)-A New Method for Speech Quality Assessment of Telephone Networks and Codecs, in: *ICASSP*, Vol. 2, 2001, pp. 749–752.
- [76] C. H. Taal, R. C. Hendriks, R. Heusdens, J. Jensen, An Algorithm for Intelligibility Prediction of Time-Frequency Weighted Noisy Speech, *IEEE Trans. Audio, Speech, Lang. Process.* 19 (7) (2011) 2125–2136.
- [77] E. Vincent, R. Gribonval, C. Févotte, Performance Measurement in Blind Audio Source Separation, *IEEE Trans. Audio, Speech, Lang. Process.* 14 (4) (2006) 1462–1469.
- [78] J. Le Roux, S. Wisdom, H. Erdogan, J. R. Hershey, SDR - Half-Baked or Well Done?, in: *ICASSP*, 2019, pp. 626–630.
- [79] S. Wisdom, J. R. Hershey, K. Wilson, J. Thorpe, M. Chinen, B. Patton, R. A. Saurous, Differentiable Consistency Constraints for Improved Deep Speech Enhancement, in: *ICASSP*, 2019, pp. 900–904.
- [80] A. Pandey, D. Wang, A New Framework for CNN-Based Speech En-



hancement in the Time Domain, *IEEE/ACM Trans. Audio, Speech, Lang. Process.* 27 (2019) 1179–1188.

- [81] Y.-J. Lu, S. Cornell, X. Chang, W. Zhang, C. Li, Z. Ni, Z.-Q. Wang, S. Watanabe, Towards Low-Distortion Multi-Channel Speech Enhancement: The ESPNet-SE Submission to The L3DAS22 Challenge, in: *ICASSP, 2022*, pp. 9201–9205.
- [82] H. Sawada, S. Araki, S. Makino, A Two-Stage Frequency-Domain Blind Source Separation Method for Underdetermined Convolutional Mixtures, in: *WASPAA, 2007*, pp. 139–142.
- [83] D. H. T. Vu, R. Haeb-Umbach, Blind Speech Separation Employing Directional Statistics in An Expectation Maximization Framework, in: *ICASSP, 2010*, pp. 241–244.
- [84] Y. Masuyama, X. Chang, S. Cornell, S. Watanabe, N. Ono, End-to-End Integration of Speech Recognition, Dereverberation, Beamforming, and Self-Supervised Learning Representation, in: *SLT, 2023*, pp. 260–265.